

THESIS FOR THE DEGREE OF DOCTOR OF PHILOSOPHY

**Interaction of Natural Organic Matter Molecules
with TiO₂ Nanoparticles: An Experimental
Adsorption and Aggregation study**

Karin Danielsson



UNIVERSITY OF GOTHENBURG

Department of Chemistry and Molecular Biology
University of Gothenburg
Gothenburg, Sweden
2018

Interaction of Natural Organic Matter Molecules with TiO₂ Nanoparticles: An Experimental Adsorption and Aggregation study

KARIN DANIELSSON

Department of Chemistry and Molecular Biology
University of Gothenburg
SE-412 96 Gothenburg
Sweden

Cover illustration: Schematic of the stabilization and destabilization of TiO₂ nanoparticles interacting with 2,3-DHBA and fulvic acid at different pH.

© Karin Danielsson 2018

ISBN 978-91-629-0515-6 (PRINT)

ISBN 978-91-629-0516-3 (PDF)

Printed in Gothenburg, Sweden 2018

Printed by BrandFactory

“The answer to one question gives rise to ten new and it seems to increase exponentially. It’s like a never ending story.”

ABSTRACT

Mechanisms by which synthetic nanoparticles are released into natural environments and the potential impact of nanoparticles on living organisms have been discussed frequently over the past decade. Interactions of nanoparticles with dissolved ions and organic ligands such as natural organic matter (NOM) affect the surface potential, which in turn may lead to aggregation of the particles, thus affecting the colloidal stability. In this study, interaction of synthetic TiO₂ (anatase) nanoparticles with various organic ligands in aqueous suspension was investigated in terms of aggregation and adsorption. Aggregation was investigated by light scattering techniques to determine ζ -potential and z-average diameter, while batch adsorption experiments were used to quantify the amount of organic ligands adsorbed onto TiO₂ nanoparticles. Size, ζ -potential and adsorption mechanisms were affected by concentration and molecular structure of the organic ligand present. Infrared (IR) spectroscopy demonstrated that inner sphere and/or outer sphere complexes were formed depending on pH and type of organic ligands in solution. In conjunction with experiments, DLVO modelling supported enhanced colloidal stability with increasing concentrations of Suwannee river fulvic acid at pH 5 compared to at pH 2.8. A combined experimental and molecular dynamic (MD) investigation of 2,3-dihydroxybenzoic acid (2,3-DHBA) and SRFA complexation showed that the extent of NP aggregation depended on concentrations of the ligand as well as on added Zn²⁺ concentrations. MD calculations showed complexation between ligands and Zn²⁺ in solution, which together with experimental adsorption and aggregation data indicated possible co-adsorption and formation of ternary surface complexes at the TiO₂ surface.

ISBN 978-91-629-0515-6 (PRINT)

ISBN 978-91-629-0516-3 (PDF)

POPULÄRVETENSKAPLIG SAMMANFATTNING

Nanopartiklar används inom nanoteknologin för att utveckla nya tekniska lösningar inom olika områden. Nano betyder miljarddel och en nanopartikel brukar definieras som en partikel med en storlek mellan 1-100 nanometer. Det unika med nanopartiklar är att ett ämne kan få nya egenskaper jämfört med samma ämne i större storlek. Forskningen brukar göra skillnad på naturliga och tillverkade nanopartiklar. Ett exempel på naturligt förekommande är frigörelsen av partiklar via askmoln som bildats efter ett vulkanutbrott medan tillverkade nanopartiklar är de som nanoteknologin utgör. Titandioxid är ett vanligt förekommande material inom nanoteknologin med flera olika användningsområden såsom vitt pigment i färg, solkräm och tandimplantat m.m. På grund av dess stora användningsområde är riskerna betydande att partiklarna slutligen når den naturliga miljön där de kan binda till naturligt organiskt material som finns i de flesta sjöar och vattendrag. Det organiska materialet kan fastna (adsorbera) på ytan av partikeln vilket i sin tur kan leda till att partiklarna blir större, man säger att de aggregerar. Denna process har betydelse för var de slutligen hamnar i naturen då stora partiklar tenderar att sjunka till botten medan små cirkulerar i vattenpelaren och är biotillgängliga för organismer som lever här. För att kunna avgöra om och hur tillverkade nanopartiklar påverkar miljön så behövs en hel del laborativa studier göras. I den här avhandlingen har jag tillverkat titandioxid nanopartiklar med en storlek på cirka 13nm och undersökt hur ytan påverkas då de interagerar med olika organiska molekyler i vattenlösning med avseende på adsorption och aggregering. Eftersom miljön är ständigt dynamisk så är de långsiktiga effekterna på omgivningen av stor betydelse. Jag har därför även undersökt eventuella effekter över både kort och lång tid i de olika systemen. Resultaten i denna avhandling visar att storlek, laddning och adsorptionsmekanismer påverkades av koncentration och molekylstruktur av de organiska molekylerna samt till viss del tid i suspension.

LIST OF PAPERS

This thesis is based on the following studies, referred to in the text by their Roman numerals.

I. **Influence of organic molecules on the aggregation of TiO₂ nanoparticles in acidic conditions**

K. Danielsson, J. A. Gallego-Urrea, M. Hassellöv, S. Gustafsson and C. M. Jonsson
J, Nanopart. Res.
19, 133 (2017)

Contribution: I performed all of the experiments (however with technical help with TEM measurements). I have contributed to the analysis and interpretation of results.

II. **Effects of the adsorption of NOM model molecules on the aggregation of TiO₂ nanoparticles in aqueous suspensions**

K. Danielsson, P. Persson, J. A. Gallego-Urrea, Z. Abbas, J. Rosenqvist and C.M. Jonsson
Nanoimpact
10, 177-187 (2018)

Contribution: I designed the concept of this study. I planned and performed all the experimental work. I performed most of the analysis and interpretation of results (however with help with interpret IR spectroscopic data). I wrote most part of the paper.

III. **Interactions of 2,3-dihydroxybenzoic acid and Zn²⁺ with TiO₂ nanoparticles: an experimental and theoretical study**

K. Danielsson, K. Kolman, Z. Abbas and C.M. Jonsson

Submitted

Contribution: I designed, planned and performed all the experimental work. I have contributed to the analysis and interpretation of results. I wrote most of the experimental part of the paper.

IV. **A comparative experimental and modelling study on aggregation and adsorption of TiO₂ nanoparticles in suspensions with SRFA and Zn²⁺**

K. Danielsson, K. Kolman, C.M. Jonsson, and Z. Abbas

Manuscript

Contribution: I designed, planned and performed all the experimental work. I have contributed to the analysis and interpretation of results. I wrote most of the experimental part of the paper.

CONTENT

ABBREVIATIONS	V
1 INTRODUCTION AND BACKGROUND	1
1.1 The development of nanotechnology	2
1.2 What are nanoparticles?	3
1.3 Possible benefits and environmental concerns of nanotechnology	5
1.4 Aim and approach	7
1.5 TiO ₂ Nanoparticles	8
1.6 Organic molecules	9
2 NANOPARTICLE INTERACTIONS	10
2.1 Point of zero charge and isoelectric point	11
2.2 Electric double layer (EDL) and ζeta-potential	12
2.3 Adsorption	14
2.4 Particle aggregation	18
2.5 Particle stabilization	20
2.6 Modeling particle suspension stability by DLVO theory	22
3 EXPERIMENTAL INVESTIGATIONS	25
3.1 Titanium dioxide nanoparticle synthesis	26
3.2 Characterization methods	27
3.3 Interaction of organic ligands with TiO ₂ NPs- analytical methods	35
3.4 Molecular Dynamic simulations (MD)	43
4 RESULTS AND DISCUSSION	44
4.1 Aggregation behaviour of TiO ₂ NPs in aquatic environment	45
4.2 Ligand adsorption onto TiO ₂ NP surface; importance of molecular structure and environmental characteristics	47
4.3 DLVO interaction energies of TiO ₂ NPs with organic ligands	53
4.4 Metal ions and nanoparticles and the formation of ternary surface complexes	55

4.5 Adsorption of 2,3-DHBA, a shift in color observation	58
4.6 Time study and the dynamic environment	59
5 CONCLUDING REMARKS.....	63
6 FUTURE PERSPECTIVES	65
ACKNOWLEDGEMENT.....	67
REFERENCES.....	70

ABBREVIATIONS

AAS	Atomic Adsorption Spectroscopy
2,3-DHBA	2,3-Dihydroxybenzoic acid
1,2,4-BTCA	1,2,4-Benzoetricarboxylic acid
DLS	Dynamic Light Scattering
DLVO	Derjaguin-Landau-Verwey-Overbeek theory
EDL	Electrical Double Layer
ELS	Electrophoretic Light Scattering
IEP	Iso-Electric Point
IS	Ionic Strength
MD	Molecular Dynamic simulation
NP	Nanoparticle
NOM	Natural Organic Matter
PZC	Point of Zero Charge
SRFA	Suwanne River Fulvic Acid
TEM	Transmission Electron Microscopy
TiO ₂	Titanium dioxide
UV-Vis	Ultraviolet-visible spectroscopy
XRD	X-Ray Diffraction

1 INTRODUCTION AND BACKGROUND

Along with new remarkable possibilities, every new technology raises concerns regarding possible negative effects on the natural environment and human health, and nanotechnology is no exception. In the first chapter of this thesis, the world of nano and the development of nanotechnology along with its numerous applications are exemplified. Also, physico-chemical properties that make nanoparticles (NPs) so unique, as well as possible environmental concerns about nanoparticles that may enter the natural environments will be discussed.

1.1 THE DEVELOPMENT OF NANOTECHNOLOGY

Nanotechnology has been given a lot of attention during the last years because of the development of new materials with wide spread applications. However, the discussion of nanotechnology and nanoparticles has been of interest for half a century and was first introduced in 1959 by Richard Feynman in his presentation “There is plenty of room at the bottom”. He described how physical phenomena changed the properties of materials depending on size and suggested two challenges in the development of these type of materials: the creation of a nano-motor and the scaling down to the desired size⁵. Today we refer these two approaches as the bottom-up and top-down methods used in nanofabrication.⁶ Maybe the big break-through in nanotechnology came in the 80’s with the development of the scanning tunneling microscope⁷, electron microscopy⁸ and the atomic force microscope.⁹ These new techniques allowed scientists to see materials at an atomic level, which was not possible in the same manner before. Along with the improvement of more powerful computers it was now possible to get insight of materials at the nanoscale.

1.2 WHAT ARE NANOPARTICLES?

What exactly are NPs and what makes them so unique? In an article by Auffman et al.¹⁰ they defined nanoparticles as:

“NPs are routinely defined as particles with sizes between 1 and 100 nm that show properties that are not found in bulk samples of the same material”.

This definition is often used of NPs and the word nano is a prefix (10^{-9}) indicating the small size of the material. There are numerous different types of nanoparticles. First, one has to distinguish between naturally occurring NPs and synthetic (man-made) NPs. Many kinds of physical and chemical natural processes produce NPs and can be found in volcanic ash cloud, ocean spray, fine sand and dust, and even biological matter. These particles have been found in the environment since ages and those are not the focus of this thesis, instead the focus is on synthetic NPs originate from nanotechnology.

NPs are generally divided into different categories depending on their size, shape and chemical properties. One type is carbon-based NPs, which are often referred to as fullerenes and carbon nanotubes (CNTs)^{11,12}. Due to the electrical conductivity, high strength and structure, fullerenes have created commercial interest.¹³ CNTs are rolled sheets of graphene and are, due to their metallic and semiconducting properties, extensively used in commercial applications as fillers, gas storage, power applications among others.^{11, 14} Another not as widely used type of material is nanoceramic, which is made of inorganic nonmetallic solids used in catalysis, photocatalysis and imaging applications.¹⁵ There are semiconductor NPs which possess unique chemical properties due to the large surface and quantum size effect and therefore show a large variation due to bandgap tuning.¹⁶ This makes them suitable in many applications such as solar cells, nanoscale electronic devices, chemical and biosensors. Metal oxide NPs, such as titanium dioxide (TiO_2), have gained a lot of attention during the past years due to use in applications such as paint and cosmetic products.¹⁷

To answer the question of what makes nanoparticle so unique, it may not be surprising that it refers to their small size. When decreasing the size to the nanometer range, it has been shown that the chemical and physical properties dramatically change compared to the bulk of the same material, and new unique properties are developed.¹⁸ An important factor is the increased specific

surface area; the smaller the particle size, the surface area per unit of mass ratio increases. This in turn leads to an increased proportion of atoms on the surface of the particles compared to inside, thereby making them chemically more reactive, and potentially altering their strength and electrical properties.¹⁹ A consequence of the large surface area per unit of mass, and the enhanced surface reactivity, nanomaterials interact with the surrounding environment more efficiently than the bulk of the same material.²⁰ Grassian et. al.²¹ showed that TiO₂ nanoparticles interact differently with oxalic acid depending on size. Another important factor that determines nanoparticle physio-chemical properties is the predominance of quantum effects. As the particle size is reduced to a few tens of a nanometer, the quantum effects are dominant, affecting the electrical, optical and magnetic behavior of the particles.²² One example is dispersed gold nanoparticles that obtained different colors depending on size. This phenomenon is explained by the motion of the electrons that are confined to different energy levels depending on the particle size, and consequently they absorb light of different wavelength and show size specific colors.²³⁻²⁵ Although NPs are made from a wide spectrum of different materials, this thesis is focused on NPs made of titanium dioxide (TiO₂).

1.3 POSSIBLE BENEFITS AND ENVIRONMENTAL CONCERNS OF NANOTECHNOLOGY

Nanotechnology has potential for large environmental benefits due to the development of new solutions to several existing environmental problems. One example is the possibility to remove pollutants such as heavy metals by sorption to nanoparticles in water treatment.²⁶⁻²⁸ Further, the development of new efficient solar cells and improved batteries may have a great positive impact in a broad environmental perspective.^{29, 30} However, the increased interest in the use of nanomaterials and their large variety of applications has generated growing concerns about the potential toxicological, health and ecological effects. As the production increases, so does the exposure to animals and humans, and the unintentional release into the natural environment. ENPs enter the environment through water, soil and air due to different human activities.³¹ In the production step, workers may be exposed to the release of small particles that may enter the cells due to inhalation or skin penetration. Leakage to the environment causes exposure to the surrounding ecosystem which may have harmful effects on animals and plants, including inflammation, genotoxicity and cytotoxicity.³² The small size of the particles along with their enhanced reactivity makes it possible to enter living cells and interact with biological systems.³²⁻³⁵ The toxicological and environmental effects of nanomaterials do not only depend on the nature or type of material, but also on the size, shape, surface modification and surface charges.³⁶ Also, the local medium and a wide range of other physico-chemical properties, as well as the continuous transformation of nanomaterials due to interactions with the surrounding controls the overall reactivity of nanoparticles in natural environments. Due to the possibility to enter and affect the environment, there have been several studies on the ecotoxicity, aggregation and transport of ENPs in recent years.^{37, 38} However, the specific and unique properties of engineered nanomaterials need to be further investigated to get a full understanding over their impact on the natural environment. For example, their mobility, bioavailability and impact on aquatic and benthic (at the bottom of oceans and lakes, including sediments) communities need to be understood. Colloidal stability of the particles (i.e. aggregation) is an important process affecting the transport and behavior of NPs in aquatic environments, where larger aggregates may lead to sedimentation³⁹⁻⁴². There are several driving

forces inducing aggregation such as pH, salinity and the presence of inorganic and organic material that interact with the particle surfaces.⁴²⁻⁴⁴ Naturally occurring ligands, such as natural organic matter (NOM) are present in most natural waters and their interaction with NPs may lead to the formation of larger aggregates⁴⁵⁻⁴⁸. Interactions of NPs with organic ligands are therefore important to study in order to determine fate, transport mechanisms and potential risk of NPs in natural environments. In addition to the organic molecules present in natural waters, different types of metal ions are also present which may interact with nanoparticle surfaces, thus affecting the colloidal stability.^{49, 50}

1.4 AIM AND APPROACH

The main objective of this thesis is to provide fundamental understanding of the colloidal stability of TiO₂ nanoparticles upon interaction with natural organic matter (NOM) molecules in aqueous suspensions. This has been investigated experimentally by systematically studying the aggregation behavior and adsorption of ligands as a function of pH and ligand-to-solid ratio to see if and how organic molecules interact with the TiO₂ surface, possibly affecting the colloidal stability of the particles. Selected phenolic carboxylic compounds were used as model substances to mimic the interactions of NPs with NOM, and standardized Suwannee River fulvic acid (SRFA) was used in order to compare with more environmentally realistic model materials. Since natural environments are highly dynamic, both short and long-term investigations were performed. DLVO theory was used to get information about the stability of the different systems. Furthermore, information regarding interactions of organic molecules with TiO₂ at the molecular level was gained by using infrared (IR) spectroscopy. In paper III and IV the aim was to investigate ternary systems with both organic ligands and Zn²⁺ ions present in the TiO₂ dispersion. These experimental results were compared with molecular dynamic (MD) simulations to gain better insight of the complexation mechanisms.

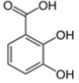
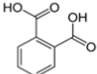
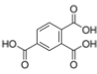
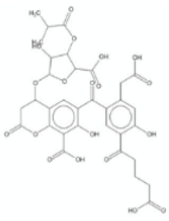
1.5 TiO₂ NANOPARTICLES

Metal oxide NPs such as titanium dioxide (TiO₂), aluminum oxide (Al₂O₃), silicon dioxide (SiO₂) and zinc oxide (ZnO), possess semiconductive and catalytical properties and are found in applications in a wide range of fields. These materials are used as pigments in paints, sunscreens, cosmetics, antimicrobial agents and in industrial operations among others.⁵¹⁻⁵⁵ TiO₂ is one of the most produced metal oxide nanomaterials, represented in about one-third of the consumer products in the nanotechnology market. Bulk materials based on TiO₂ have been massively produced and widely used as a white pigment for many years. In the last decades, nanosized TiO₂ has been introduced in a number of commercial products such as cosmetics, sunscreens, toothpaste, and as a food additive.^{40, 56} They are also used for environmental purposes to decontaminate soil and water through the adsorption of heavy metals.⁵⁷ TiO₂ nanoparticles become photoactivated under near-UV light and reactive oxygen species (ROS) are formed on the particle surface.^{58, 59} This photocatalytic property of TiO₂ NPs has been used in environmental technology for wastewater treatment, the removal of organic compounds and the degradation of air pollutants.⁶⁰ TiO₂ exists in three main crystallographic structures, anatase, rutile and brookite, each form with different properties and therefore different applications. The structure of anatase and rutile is tetragonal, while brookite has an orthorhombic configuration. The crystal structure of rutile consist of TiO₆ octahedrons with two sharing edge oxygen pairs and eight corner oxygen atoms. While the octahedron in the anatase structure has four share edges and four share corners. Another difference is that the Ti-Ti distance for rutile is shorter, while the Ti-O distance is longer than in anatase. The orthorhombic structure of brookite consists of TiO₆ octahedra with three sharing edges.^{61, 62} The different crystalline structures of TiO₂ seem to have different toxic impact. Anatase was shown to be 100 times more toxic than rutile, which might be due to the fact that anatase is more effective in generating ROS.⁶³⁻⁶⁶ The wide use of TiO₂ NPs in consumer products have raised the concern of their leakage into the natural environment, which leads to increased environmental exposure of TiO₂ NPs. More studies are therefore necessary in order to investigate the possible negative environmental impact.

1.6 ORGANIC MOLECULES

Natural organic matter (NOM) is a complex mixture of thousands of organic compounds present in most natural waters. NOM molecules contain several different functional groups, such as phenolic, carboxylic and hydroxyl groups and may have significant hydrophobic properties.⁶⁷ Nanoparticles may interact with NOM influencing the stability and aggregation of the particles.^{45, 68} In this study standardized Suwannee river fulvic acid (SRFA) was used to investigate the interactions with TiO₂ NPs in aquatic environments. Additionally, three smaller ligands were chosen in order to investigate the influence of type and position of functional groups on the aggregation behavior of TiO₂ NPs. The organic ligands used in this study are 2,3-dihydroxybenzoic acid (2,3-DHBA), phthalic acid, 1,2,4-benzoetricarboxylic acid (1,2,4-BTCA), and SRFA, and are presented in Table 1.

Table 1 Molecular structures of organic model molecules with corresponding pK_a values. (modified from paper II and IV).

	2,3-DHBA	Phthalic acid	1,2,4-BTCA	SRFA	SRFA DFT
Structure					
M _w (g/mol)	154.12	166.13	210.14	551	
pK _{a1}	2.93	2.98	2.52	3.76	2.15
pK _{a2}	10.07	5.28	3.84	9.84	3.81
pK _{a3}	N/A	-	5.20	N/A	4.16
pK _{a4}	-	-	-	N/A	5.10

2 NANOPARTICLE INTERACTIONS

In nanotechnology particle stabilization is of high importance to achieve different properties of the material, since the particle size has a large impact on surface interactions, i.e. smaller particle size leads to higher surface energy. A particle suspension is often considered stable when there are no significant variations in size and charge of particles over time. By stabilization of particles in different modes one can prevent them to form larger aggregates and in that way keep particles suspended. Stabilization of nanoparticles can be achieved by controlling several different factors such as change in pH, ionic strength, temperature and interaction with other compounds. The following chapter describes mechanisms that control aggregation and colloidal stability of particles.

2.1 POINT OF ZERO CHARGE AND ISOELECTRIC POINT

Particle surfaces possess a local charge which may be positive or negative and arises from chemical reactions at the surface i.e. adsorption of ions or protonation/deprotonation. The charged surface of particles generates an electric field, which can accumulate charged species of opposite sign and repel of same sign. Particle charges are dependent on proton transfer, i.e. pH, of the dispersion where high pH makes formation of a negatively charged surface and consequently at low pH a positively charged particle surface is obtained. pH at the point of zero charge (pzc) is the pH where the surface has a net charge equal to zero, i.e. the surface is neutral. pH_{pzc} for TiO_2 (anatase) is 6-6.5 and the surface will be positively charged at solution pH values less than the pH_{pzc} , and thus be a surface on which anions may adsorb.^{3, 45} The pH_{pzc} is determined by potentiometric titrations. In comparison, the isoelectric point (IEP) corresponds to the pH where the overall potential is zero or, more specific: the pH in a colloidal suspension at which the solute does not move in an electrophoretic field. The IEP is normally determined by ζ -potential measurements.⁶⁹ Although these two parameters are not theoretically the same it is not uncommon that they coincide to the same pH value, especially in solutions containing non-adsorbing ions.⁷⁰

2.2 ELECTRIC DOUBLE LAYER (EDL) AND ZETA-POTENTIAL

A metal oxide surface in contact with water is, in practice, charged, most often due to protonation or deprotonation depending on pH. This gives rise to a surface potential that is further balanced by the adsorption of counter ions from the solution. This layer of counter ions is called the Stern layer and beyond the Stern layer there are both positive and negative ions in what can be considered as a “cloud of ions” and more specifically diffuse layer. Together they form the so-called electrical double layer (EDL) at the particle-liquid interface and the thickness of the EDL is determined by the Debye length, $1/\kappa$. (Fig.1) The Stern layer in EDL consists of a layer with counter-ions in contact with the charged surface that are electrostatically attracted to the surface.⁷¹⁻⁷³ Here only non-specific adsorption occurs. There are only weak attractive forces and the counter-ions, which retain their hydration sphere, can come no closer to the surface than the Stern plane. The diffuse plane, also named the Gouy layer for planar surfaces, is affected by the surface potential and the thickness depends on the ionic strength of the solution. Specific adsorption may also occur to such large extent that charge reversal is obtained in the inner Helmholtz plane (IHP) according to the triple layer model where EDL is divided into inner, outer Helmholtz planes and a diffuse layer.⁷⁴ Here the potential from the counter ions are larger than the original surface charge. Charge reversal may occur when for instance an excess of anions have adsorbed to a positively charged particle. The suspended particle would instead behave as a negatively charge particle. This would in turn lead to specific or non-specific (electrostatic) adsorption of cations. The potential decay in the Gouy layer would result from a relative abundance of cations rather than anions. In a particle suspension, modification of the particle surface may be required to avoid aggregation. By the adsorption of macromolecules such as polymers to the surface of the particles, steric stabilization can be obtained.^{73, 75, 76}

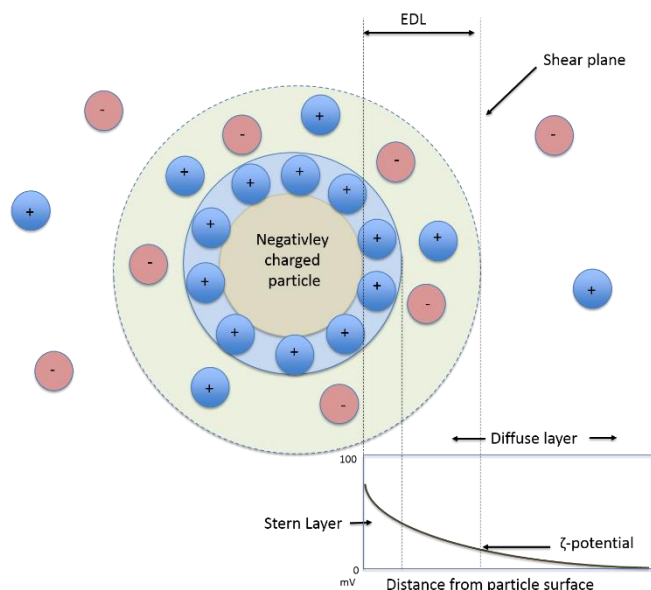


Figure 1 Schematic representation of the electric double layer around the negatively charged particle. Modified from Kaszuba *et al.*²

ζ -potential is a physical property that is referred to as the electrical potential at the shear plane of a dispersed particle and Figure 1 illustrates the position of the shear plane and ζ -potential relative to the surface of the particle. One of the most important factors that affect the ζ -potential is the pH of the bulk solution but also the ionic strength, concentration of molecules such as organic ligands, and the temperature.^{77, 78} ζ -potential is a useful and important parameter to determine the stability of a particle and colloidal suspension. Suspensions involving particles obtaining high (positive or negative) ζ -potential values ($\pm 30\text{mV}$) are electrostatically stable, while particles with low values lead to destabilization of the system and tend to aggregate^{79, 80}.

2.3 ADSORPTION

Adsorption of molecules onto the surface of nanoparticles modifies surface properties. Adsorption is therefore a key process to investigate in order to determine the fate of nanoparticles in natural environments. In this thesis the adsorption behavior was studied experimentally using batch adsorption experiments. To get information at the molecular level, i.e. inner- or outer-sphere complexation, infrared (IR) spectroscopy was used.³ Results from experiments were compared with Langmuir and Freundlich isotherm models.

2.3.1 INNER SPHERE AND OUTER SPHERE COMPLEXES

Adsorption of a molecule on a particle surface can occur in three different ways. One is chemisorption where coordinative bonds between metal and ligand at the surface are formed. Another is physio-sorption, which occurs through electrostatic interactions and van der Waals attractive forces.^{81, 82} Additionally, hydrophobic adsorption may also occur when a hydrophobic ligand adsorbs to the surface because they are repelled by the surrounding water molecules.⁸³ At a metal oxide surface, such as TiO_2 , the oxygen and metal ion possess partial charges. This means that mineral surfaces in aquatic environments attract and bind water molecules, building up a surface charge. Surface complexes may be divided into inner sphere or outer sphere complexes. Inner sphere complexes (chemisorption) involve the formation of a covalent bond to some degree between the adsorbed species and the surface. Outer sphere complexes are driven by electrostatic interactions (physiosorption) and formed by water molecules in between the surface and adsorbed organic ligand or metal.^{82, 84} (Fig.2)

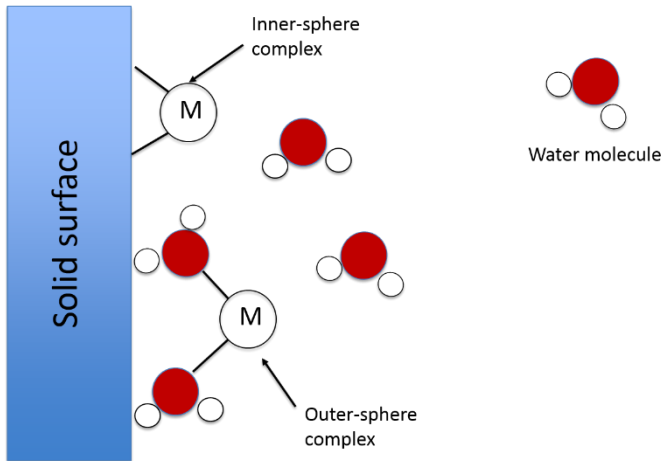


Figure 2: Schematic illustration of the formation of inner-sphere and outer-sphere complexes at the solid–water interface. Modified from Stumm et al (1995).¹

2.3.2 LANGMUIR AND FREUNDLICH ADSORPTION ISOTHERMS

Adsorption models such as Langmuir and Freundlich adsorption isotherms have been widely used for the evaluation of adsorption phenomena.⁸⁵⁻⁸⁷ The adsorption of organic ligands on solid surfaces results in the formation of monolayer or multilayers. If the best fit to experimental data is obtained by the Langmuir model, the adsorption layer consists of a monolayer while Freundlich isotherm describes a multilayer adsorption with the assumption that multilayers are formed by non-interacting monolayers.^{87, 88} The Langmuir adsorption model can be described by the following equation:

$$\frac{C_e}{q_e} = \frac{1}{q_m b} + \frac{C_e}{q_m} \quad (1)$$

where C_e is the concentration of adsorbate remaining in the solution at equilibrium (mg/L); q_e is the amount of ligand adsorbed by a unit mass of the particle at equilibrium (mg/g); q_m is the maximum adsorption capacity (mg/g) and b is the Langmuir adsorption constant (L/g). The Freundlich adsorption model was given in the equation below:⁸⁹

$$\ln q_e = \frac{1}{n} C_e + \ln k_f \quad (2)$$

Where k_f is the Freundlich constant and $1/n$ is the intensity of adsorption.

In this study we have used these models in paper II and III in order to get additional understanding of the adsorption mechanisms of organic ligands on the TiO₂ particle surface.

2.4 PARTICLE AGGREGATION

In a suspension, particles are in constant motion caused by molecular collisions, a phenomenon known as the Brownian motion. Brownian motion is the random movement of solvent molecules due to thermal energy which in turn causes the particles to move.⁹⁰ Depending on size, particles will be affected differently by the Brownian motion, where small particles are more affected than larger ones. Collisions between nanoparticles may form aggregates larger than the primary particles, a process named aggregation.⁹¹ Particle aggregation is generally considered a two-step process where particles collide and collisions may lead to attachment. Aggregation of particles affects the overall properties of the particle, which significantly influences the colloidal stability of the system.⁹² The colloidal stability of particles in suspension is primarily affected by pH, dissolved electrolytes and organic molecules present in the media.⁹³ When increasing pH the particles tend to aggregate due to a decreased surface charge and subsequent decrease in repulsive forces making the particles collide and attach to each other (Fig 3a). When increasing the ionic strength the diffuse double layer is compressed and the repulsive forces between the particles decreases. A decrease in repulsive forces may in turn lead to aggregation and the formation of larger particles..^{42, 43} In this study the ionic strength was kept constant at 10 mM (paper I-IV). In one experiment 200 mM NaCl was used to investigate the effect of ionic strength upon aggregation and preliminary results showed that the particles formed larger aggregates than at 10 mM NaCl (Fig 3b). Additionally, interactions of TiO₂ with organic ligands may also induce aggregation and thus affect the colloidal stability by influencing the surface charge.^{3, 4} Figure 3c (modified from paper I) shows the aggregation behavior of 2,3-DHBA in the presence of TiO₂ NPs at pH 2.8 where increased concentration of 2,3-DHBA gave rise to larger aggregates. Similarly, humic and fulvic acids have also been shown to affect the aggregation behavior of NPs depending on ligand concentration.^{4, 47, 94, 95}

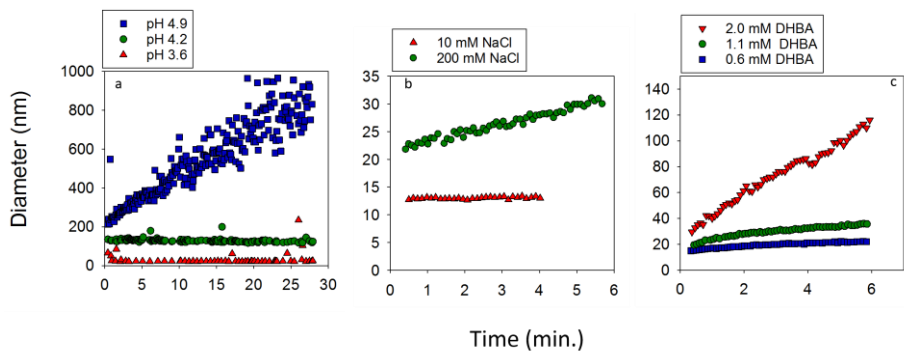


Figure 3 Hydrodynamic diameter as a function of time followed by DLS at a) different pH b) different concentration of NaCl and c) different concentration of 2,3-dihydroxybenzoic acid (2,3-DHBA)(modified from paper 1). Particle concentration was 0.1 g/L and temperature 20°C

2.5 PARTICLE STABILIZATION

There are different approaches to prevent particle aggregation in aquatic suspensions, electrostatic repulsion and steric hindrance. Electrostatic repulsion is caused by the surface charge on particle surfaces. Particles with equal charge repel each other which results in a stable system. For particles that are uncoated, electrostatic repulsion is the primary stabilization mechanism.^{96, 97} Steric stabilization is achieved through the sorption of molecules onto the particle surface (Figure 4). The molecules attached to the surface often exhibit one polar and one nonpolar end keeping them away from each other due to the reduction of the attractive van der Waals forces.

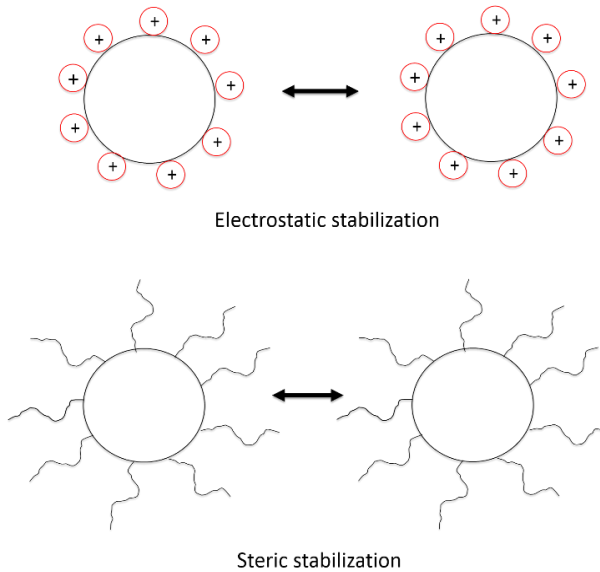


Figure 4 Schematic presentation of electrostatic and steric stabilization of nanoparticles.

2.5.1 STERIC STABILIZATION INDUCED BY NOM

Aquatic and soil environments are enriched with natural organic matter (NOM) with a variety of structures and compositions, including humic and fulvic acids. It has been shown that NOM-type molecules can affect the aggregation behavior of NPs in suspension^{94, 95} An increased stabilization in the presence of NOM is thought to be due to steric stabilization mechanisms in which the adsorbed NOM molecules prevent the particles to approach each other and stick together. It has also been shown that these interactions were caused by electrostatic stabilization as the surface charge of the particles with attached NOM molecules increased.^{45, 94, 98-100} Similar phenomena was also observed in this study (Paper I and II) where an increase in SRFA concentration gave rise to charge inversion and the formation of smaller aggregates.^{3, 4}

2.6 MODELING PARTICLE SUSPENSION STABILITY BY DLVO THEORY

In this thesis, classical Derjaguin-Landau-Verwey-Overbeek (DLVO) theory was used to understand to which extent electrostatic repulsion contributed to the colloidal stability of the systems studied. DLVO theory was first described in 1943 and is frequently used to estimate the total interaction energy between particle surfaces and interacting molecules or ions.^{101, 102} The theory describes the interactions between colloids in the sense of two interactions, a repulsive electrostatic force (V_{EDL}), which arises due to charge on the surface of the particle and a van der Waals attractive force (V_{vdW}). By combining these two forces, the DLVO potential is obtained. This potential provides information of the stability of the system and may explain why some particles tend to aggregate while others do not.¹⁰³(Eq 3; Figure 5)

$$V = V_{vdW} + V_{EDL} \quad (3)$$

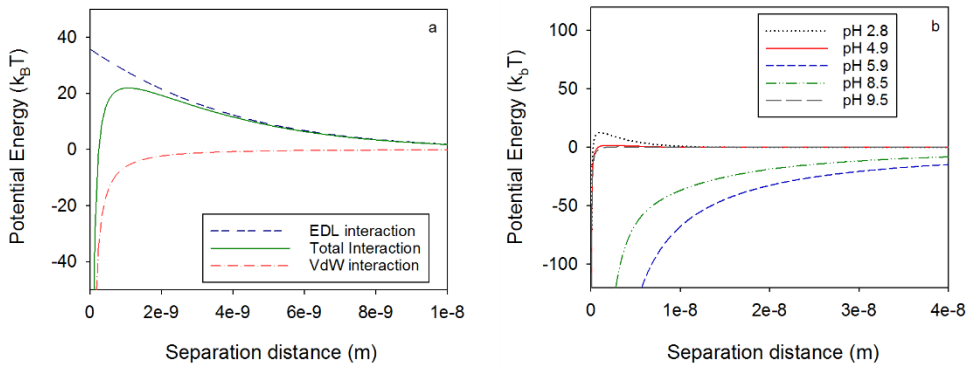


Figure 5 Energy profiles (a) and DLVO interaction energies of bare TiO₂ nanoparticles (b) (modified from paper 2)³

The van der Waals attractive forces refer to several categories of interactions that originate from interactions at the molecular level. In general, three types of interactions are classified as vdW interactions, Keesom interaction that accounts for permanent dipole interactions; Debye interaction for -induced dipole interactions; and London interaction for dipole- dipole interactions.¹⁰⁴ Unlike the Keesom and Debye interactions that require the presence of permanent dipoles, the London interaction is universal. The theoretical descriptions of these three types of forces all reveals a dependence on separation distance to the power of sixth. The van der Waals attractive interaction is determined according to the following expression:

$$V_{vdW} = -\frac{A}{6} \left[\frac{2a^2}{s(4a+s)} + \frac{2a^2}{(2a+s)^2} + \ln \frac{s(4a+s)}{(2a+s)^2} \right] \quad (4)$$

Where A is the Hamaker constant of TiO₂ in water (3.5*10⁻²⁰ J) and was obtained by Gomez-Merino et al ¹⁰⁵, a is the radius of the two particles (z-average radius) separated by a distance between surfaces, s.

Electrostatic double layer repulsive force becomes significant when the electrostatic double layer from two particles interfere. To overcome this repulsion the system requires energy. The electrostatic double layer interaction, V_{EDL}, is determined according to the following expression:

$$V_{EDL} = 2\pi\epsilon a\zeta^2 \ln(1 + e^{-Ks}) \quad (5)$$

$$K = \sqrt{\frac{e^2 \sum_i c_i z_i^2}{\epsilon \epsilon_0 k_B T}} \quad (6)$$

where $\epsilon = \epsilon_r \epsilon_0$ is the dielectric constant. ϵ_r is the dielectric constant of water (80.19 at 20°C)¹⁰⁶, e is the elementary charge, c_i is the concentration of the electrolyte and z_i its valency, k_B is the Boltzmann constant, and T is the absolute temperature. The V_{EDL} potential corresponds to the Derjaguin

approximation between two spheres with equal charge. K is the inverse Debye length. As seen from equation 6, an increased ionic strength in the suspension causes a decreased surface potential. As a consequence, the EDL is compressed. This means that the repulsion energy as well as the energy barrier decreases. If the repulsion energy is reduced to an extent that causes the energy barrier to disappear, every collision between particles will lead to aggregation.

3 EXPERIMENTAL INVESTIGATIONS

TiO₂ NPs used throughout this thesis were synthesized from hydrolysis of TiCl₄ according to a well-developed method¹⁰⁷ and used as model particles. Monodispersed particles with an average particle size of 13 nm (± 1 nm) were synthesized and characterized by several analytical methods. The synthesis process and characterization methods are explained in more detail below.

3.1 TITANIUM DIOXIDE NANOPARTICLE SYNTHESIS

TiO₂ NPs were synthesized by the controlled hydrolysis of TiCl₄ (Fig. 6a). Dialysis against ultrapure (Milli-Q) water was done to reduce the concentration of Cl⁻ ions and to increase pH of the colloidal suspension and thereby minimize particle aggregation. Both dialysis and storage were performed at 20°C.

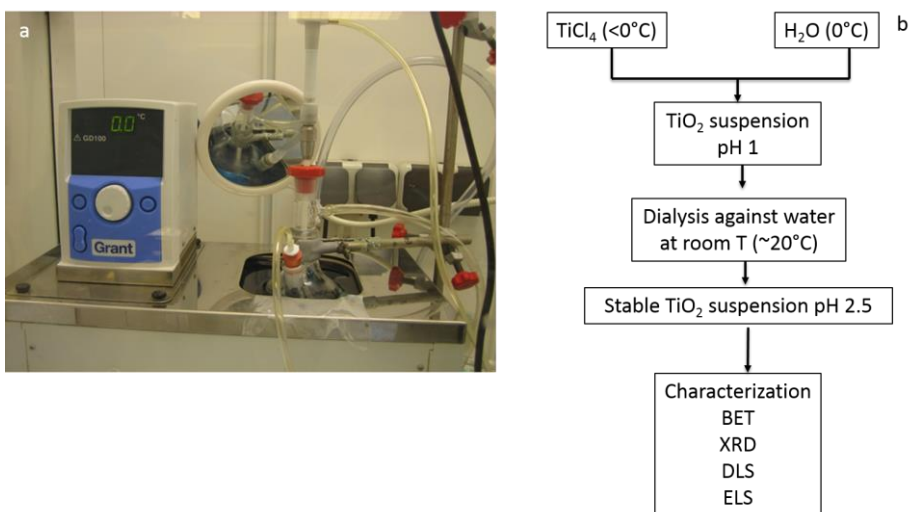


Figure 6 Experimental set-up for TiO₂ NP synthesis (a) and schematic theme of the synthesis process. (b) The reacting solution is kept at 0°C and under continuous stirring.

3.2 CHARACTERIZATION METHODS

The synthesized TiO₂ particles were characterized with several different analytical techniques including:

- X-ray diffraction (XRD)
- Nitrogen adsorption (BET)
- Dynamic Light Scattering (DLS)
- Electrophoretic Light Scattering (ELS).

3.2.1 BET SPECIFIC SURFACE AREA - NITROGEN ADSORPTION

The Brunauer-Emmet-Teller method (BET) method is a technique commonly used to determine the specific surface area of metal oxide particles through the adsorption of nitrogen at the temperature of liquid nitrogen, ~ 77 K, at different pressures. By a stepwise increase in the relative pressure over the surface, N_2 gas molecules will be adsorbed on the surface and a plot of the amount adsorbed versus the relative pressure is made, called an isotherm. From the isotherm it is possible to get information about the surface porosity.¹⁰⁸ The specific surface area is presented as surface area per unit of mass (m^2/g).

In this thesis, results from the BET measurements were used for calculating the adsorption of ligands and metal ions to the particle surface. Results were normalized to surface area, thus amounts of adsorption is presented in the unit $\mu\text{mol}/m^2$. It is worth mentioning that different batches of synthesized TiO_2 particles had a small variation in BET specific surface area, ranging from 157-206 (m^2/g). The same batch of particles throughout one specific study was used (one batch in paper I, another in paper II, and a third batch in paper III and IV). In each case, the correct BET value was used for the specific batch.

3.2.2 X-RAY DIFFRACTION (XRD)

X-Ray diffraction is an analytical technique primarily used to obtain information about the structure of crystalline materials. Since TiO_2 has three different crystalline forms, all with different properties that may affect the colloidal stability in dispersed media, it was of high interest to investigate the chemical composition of the material. Sample preparation was done by drying the particle suspension at 70°C in an oven overnight and then ground to fine powder. By using a gradually rotated monochromatic X-ray beam to bombard the sample, a diffraction pattern is obtained. The diffraction pattern is described by Bragg's Law (Fig.7):

$$2d\sin\theta = n\lambda$$

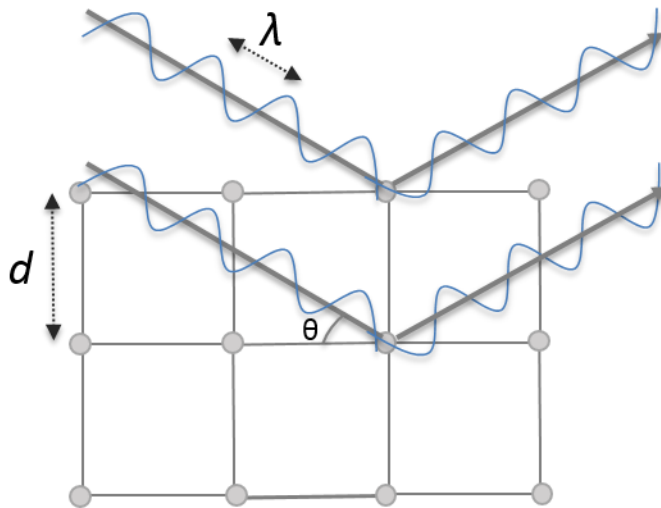


Figure 7. Illustration of Bragg diffraction of X-rays according to Bragg's law.

Since each crystalline phase yields a characteristic diffraction pattern it is possible to identify different crystalline phases, almost like fingerprinting. The results from XRD showed predominance of anatase phase present in the synthesized TiO_2 NPs with some contribution (<10%) of brookite, which was consistent with a former study by Abbas et al (2011)¹⁰⁷ and results are shown in figure 8.

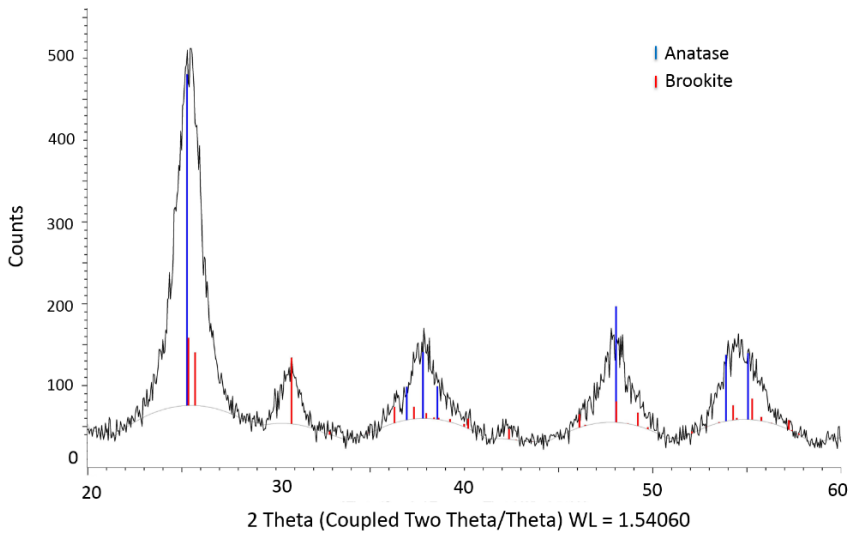


Figure 8 XRD data of synthesized TiO_2 NP showing that Anatase is the dominant crystal structure.

3.2.3 DYNAMIC LIGHT SCATTERING (DLS)

Dynamic light scattering (DLS) is a technique used for studying size of colloidal dispersions of particles. When light hits small particles the light scatters in all directions (Rayleigh scattering). In DLS the particles are illuminated with a laser beam where the intensity of the scattered light fluctuates over short timescales at a rate that is dependent upon the size of the particles; smaller particles move more quickly and are displaced further by the molecules in the solvent (Fig. 9). It is possible to record the temporal variations of the scattered light. These fluctuations are due to the fact that the small molecules in solutions are undergoing Brownian motion and so the distance between the scatters in the solution is constantly changing with time. These temporal variation is caused by dynamical properties of the system, for instance by the motion of dispersed particles.¹⁰⁹ The dynamic information of the particles is derived from an autocorrelation of the intensity trace recorded during the experiment given by:

$$g^2(q, t) = \frac{\langle I(\tau)I(\tau+t) \rangle}{\langle I(\tau)^2 \rangle} \quad (7)$$

Where I is the intensity, τ is the time, t the delay time. The magnitude of the scattering vector q is given by:

$$q = \frac{4\pi n}{\lambda} \sin\left(\frac{\theta}{2}\right) \quad (8)$$

Where n is the refractive index of the solvent, λ is the wavelength of the incident beam and θ the angle of detected light.

Light scattering is a mechanism of absorption and re-emission of electromagnetic radiation. The velocity of the brownian motion of particles in dispersion is defined by the translational diffusion coefficient (D).¹¹⁰ Analysis of the intensity fluctuations gives the brownian motion and also the particle size, hydrodynamic diameter (d_H), using the Stokes-Einstein equation:^{111, 112}

$$d(H) = \frac{kT}{3\pi\eta D} \quad (9)$$

Where k is the Boltzman constant ($1.38 \times 10^{-23} \text{ m}^2 \cdot \text{kg} \cdot \text{s}^{-2} \cdot \text{K}^{-1}$), η is the viscosity of the medium and D is the diffusion coefficient.

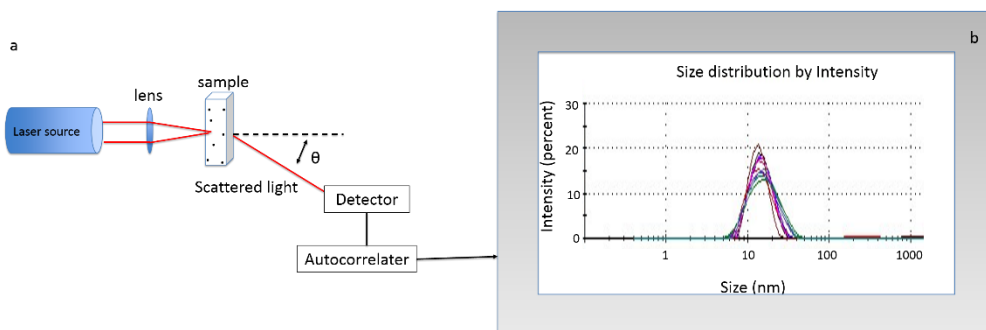


Figure 9 Schematic illustration of the DLS set-up (a) and snapshot from size distribution of TiO_2 nanoparticles at pH 2.8 (b).

Dynamic light scattering has in this thesis been used to follow the initial aggregation of particle dispersions, as well as measure the hydrodynamic diameter to get an understanding of the colloidal stability of TiO_2 when interacting with different molecules. All data presented from DLS measurements throughout this thesis is the z-average diameter.

3.2.4 ELECHROPHORETIC LIGHT SATTERING (ELS)

Electrophoretic light scattering (ELS) was used to determine ζ -potential of particle suspensions. The electrophoretic motion of charged particles in an external applied field can be followed, making it possible to determine the ζ -potential of dispersed particles. It can be defined as the electrical potential of a charged particle at the shear plane, where the magnitude of the ζ -potential indicates the stability of the colloidal system. This means that if the absolute value of the ζ -potential is large ($>+30\text{mV}$ or $<-30\text{mV}$) then the particles in suspension will be electrostatically stabilized and collisions between particles will not lead to an aggregation. It is assumed that the ζ -potential corresponds to the Stern-layer potential. Measurement of the ζ -potential is actually the determination of the electrophoretic mobility, which is converted to ζ -potential by some theoretical model such as Smoluchowski or Henrys approximations depending on the size and the ionic strength of the media (eq.10)^{112, 113}.

$$u = \frac{2\varepsilon\varepsilon_0\zeta}{3\eta} f(\kappa a) \quad (10)$$

where ε_0 is the permittivity in vacuum $8.85 \cdot 10^{-12} \text{ C}^2/\text{J}$, ε is the relative permittivity for the solution (80.1 at 293K), ζ is the ζ -potential η is the viscosity of the medium and a is the radius of the particle and κ the Debye Hückel parameter^{113, 114}:

$$\kappa = \sqrt{\frac{\sum_i((n_i)_0 \cdot z_i^2) \cdot e_0^2}{\varepsilon \cdot \varepsilon_0 \cdot k_B \cdot T}} \quad (11)$$

where $(n_i)_0$ is the concentration if the i^{th} ion in the bulk phase and z_i is its valence, e_0 is the elementary charge ($1.602 \cdot 10^{-19} \text{ C}$) and T is the temperature.

Equation 13 was used in calculating ζ -potentials with the correction term $f(Ka)$ given by the Oshima's equation (eq.15).¹¹⁴ If the z-average diameter of the particles is larger than 200 nm then equation 12 approaches Smoluchowski approximation, otherwise it becomes Henry's equation with $f(\kappa a)$ approaching 1.5.

$$f(Ka) = 1 + \frac{1}{2\left(1 + \frac{2.5}{Ka(1+2ee^{-Ka})}\right)^3} \quad (12)$$

Electrophoretic light scattering was in this thesis used to investigate the colloidal stability of TiO₂ NPs when interacting with different molecules. In combination with DLS data it gave important and valuable information about the different systems investigated. The same instrument (Zetasizer Nano) as used for DLS measurements was also used for ζ -potential determinations but with a different sample cell.

3.3 INTERACTION OF ORGANIC LIGANDS WITH TiO₂ NPS- ANALYTICAL METHODS

When further investigated the interaction behavior of organic ligands and Zn²⁺ with the particle surface, several additional techniques were used such as:

- Transmission Electron Microscopy (TEM);
- Infrared Spectroscopy (IR);
- UV-Vis spectroscopy
- Atomic Adsorption Spectroscopy (AAS).
- DLS and ELS described above were used frequently throughout the entire thesis.

3.3.1 TRANSMISSION ELECTRON MICROSCOPY (TEM)

In this thesis transmission electron microscopy (TEM) was used to get further insight into particle size and shape of TiO₂ when interacting with 2,3-DHBA and phthalic acid at pH 2.8 and results are presented in paper I.

Electron microscopy is similar to optical spectroscopy with the exception of using electrons instead of photons. Free electrons from an electron gun are accelerated in a high voltage potential in a high vacuum environment to avoid collisions and any kind of interactions between the electrons and other particles. Then the upper electromagnetic condenser lenses of the TEM induce the beam formation and the electrons are then guided to the sample. The incident electrons can interact in several ways with the sample resulting scatter or backscatter elastically or in-elastically scattered electrons, which can be used to gain different types of information. Then the beam after passing through and interacting with the sample reaches a fluorescent screen, resulting in a 2D projection^{115, 116}.

In order to let the electrons pass through the sample, it has to be very thin and dry. Sample preparation is therefore a crucial and important step. Since our particles are in dispersion, air-drying was conducted by directly placing one drop of the sample on the TEM-grid and dry overnight before analyzing.

3.3.2 INFRARED SPECTROSCOPY (IR)

Molecules contain an amount of energy that is distributed throughout their structure making vibrations to occur. Bonds are not actually fixed; the bonds are constantly changing in length due to these vibrations. The amount of energy a molecule contains is quantized i.e. it can only bend and stretch at specific frequencies which correspond to specific energy levels. In infrared (IR) spectroscopy a sample is irradiated with electromagnetic radiation resulting in absorption of radiation at a certain frequency specific to the molecular motion of the molecule.

By measuring the IR spectrum it is possible to find out what kind of motion is occurring and by interpreting those motions one can determine what kind of functional groups that are present in the molecule. The IR range of the electromagnetic spectrum is above the visible, 7.8×10^{-7} to about 10^{-4} m. The wavelength in the IR region is often given in micrometer (μm) and the frequencies in wavenumber (cm^{-1}).

$$\text{Wavenumber: } \tilde{\nu} (\text{cm}^{-1}) = \frac{1}{\lambda(\text{cm})} \quad (13)$$

This technique is very complex since a lot of organic molecules contain several different functional groups which in turn leads to many different vibrations due to bond stretching and bending motions. An IR spectrum with several different absorption peaks is achieved and every molecule is unique. One can say that an IR spectrum represents a fingerprint of a sample where most functional groups have specific IR absorption bands making it possible for identification. By comparing spectra of the ligand in aqueous solution at different protonation states to spectra of the surface at which the ligand has adsorbed, information

can be obtained on which functional groups are involved in the surface interactions, as well as the degree of protonation of the surface complexes.

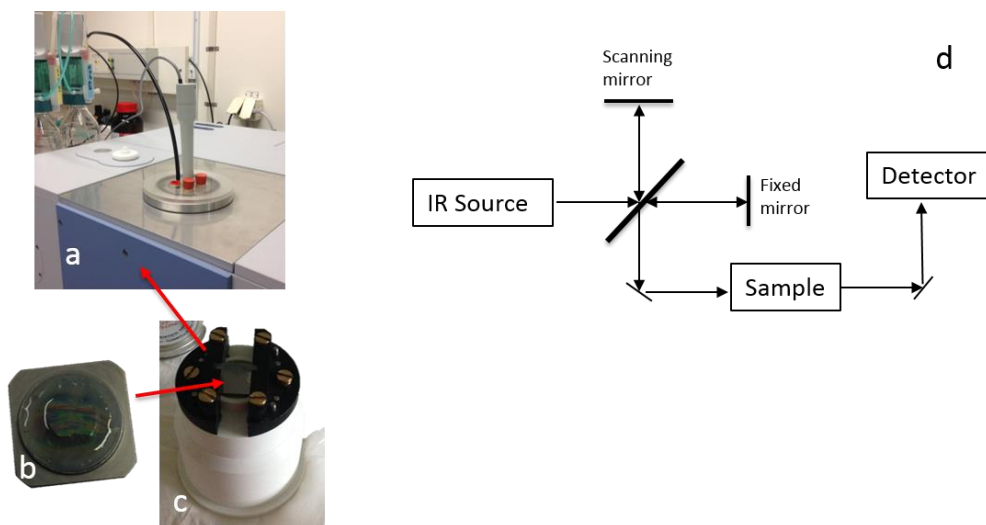


Figure 10 To the left; Instrumentation set-up of IR spectroscopy (a) with Ge crystal doped with TiO_2 NP suspension (b) placed in the sample vessel (c.) To the right; schematic illustration of the instrumentation (d).

3.3.3 BATCH ADSORPTION EXPERIMENTS

To gain better understanding of the mechanisms behind the aggregation behavior of TiO₂ NPs in the presence of organic molecules (table 1) and Zn²⁺, batch adsorption experiments were performed. Samples were kept on a rotator during the whole experiment (Fig. 12). After certain time (10-min up to days and weeks) the samples were transferred to centrifugation tubes and ultracentrifuged. The concentration of the respective organic molecule in the supernatant (remaining in solution) was determined by UV-Vis spectrophotometry, while the amount of Zn²⁺ was measured and determined with atomic absorption spectroscopy (AAS).

Adsorption data was displayed as μmol/m² and as % adsorption and was calculated according to following expressions:

$$C_{adsorption} = C_{total} - C_{solution} \quad (14)$$

$$Adsorption \left(\frac{\mu\text{mol}}{\text{m}^2} \right) = \frac{C_{adsorption}}{C_{particle} * BET} \quad (15)$$

$$\% Adsorption = \frac{C_{adsorption}}{C_{total}} * 100 \quad (16)$$

Where C_{total} corresponds to total ligand concentration, C_{sol} is concentration left in solution after particles have been removed from the suspension, and C_{ads} is removal from solution, assumedly adsorbed to the surface.

In paper II-IV all samples were covered with aluminum foil to avoid any interference with light and also kept on a rotator during the whole experiment (Fig. 11).



Figure 11 Samples on rotator covered with aluminum foil to avoid interaction with light.

Ultraviolet-visible spectroscopy (UV-Vis)

Ultraviolet-visible spectroscopy (UV-Vis) is a commonly used analytical method for quantitative determinations. In UV-Vis spectroscopy, samples are put into a cuvette which is illuminated with light of wavelength of ~200-800 nm. The UV light or visible radiation is absorbed by the sample in the cuvette. For each wavelength the intensity of light is passing through a reference cell (I_0), and the sample cell (I) and the absorbance (A) of the sample is related to I and I_0 according to:

The amount of absorbed radiation depends on the concentration of the sample, the path length of the light and the possibility for the sample to absorb the light at a certain wavelength. According to the Beer-Lamberts Law the absorbance

$$A = \log \frac{I_0}{I} \quad (17)$$

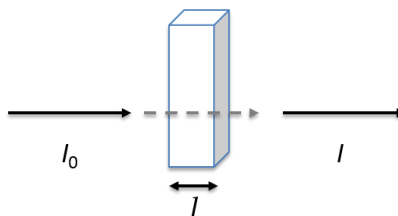


Figure 12 Illustration of the radiation coming in (I_0) and radiation coming out (I)

(A) is proportional to the concentration of the sample according to:

$$A = \epsilon cl \quad (18)$$

where ϵ is molar extinction, c is the concentration and l is the path length. All samples were acidified and a new calibration curve was performed before each analysis.

Atomic Adsorption Spectroscopy (AAS)

In paper III and IV, investigations of ternary systems were performed to find the amount of Zn^{2+} adsorbed to the particles. Atomic absorption spectroscopy (AAS) is a technique for detecting metals or metalloids in a sample and the total concentration of a metal in solution is obtained. The adsorption of Zn^{2+} was measured with AAS with a zinc hollow cathode lamp as radiation source. The lamp consists of a tungsten anode and the cathode is made of the same element to be determined, in this case zinc. In the nebulizer, the sample is converted into a fine aerosol that is introduced to the flame. The next step, the atomization, is to convert the analyte to free gaseous atoms which is done by exposing the analyte to high temperature in the flame. A monochromator is used to disperse the incident light beam and making it possible for the selected wavelength to reach the detector.^{117, 118} The zinc concentration remaining in solution in each sample was calculated using Beer-Lamberts law explained in the UV-Vis section above.

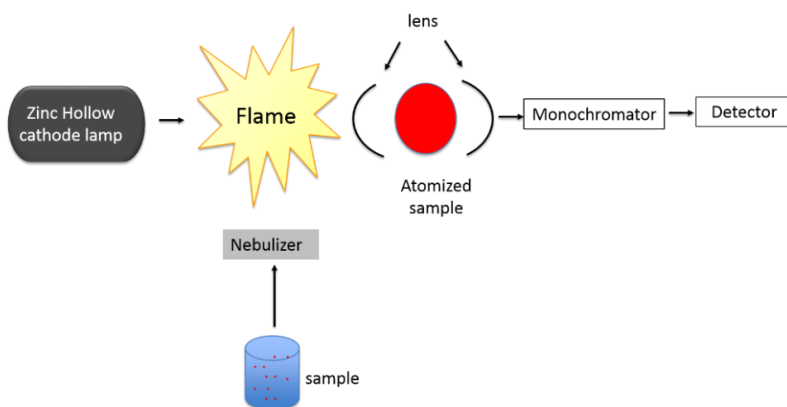


Figure 13 Schematic diagram of AAS set-up.

3.4 MOLECULAR DYNAMIC SIMULATIONS (MD)

Molecular Dynamics simulation is a computational technique that can be used to gain better understanding of molecular interactions in bulk solutions. MD simulations were performed using the software of GRONingen MACHine for Chemical Simulation (GROMACS) ¹¹⁹ and the CHARMM general force field was used for bonded and non-bonded interactions in the system. ^{120, 121} In this thesis MD was used to get information of the complexation between SRFA and 2,3-DHBA respectively with zinc. The calculated results obtained from the simulations were used to compare with experimental results and are presented in papers III and IV.

4 RESULTS AND DISCUSSION

In this thesis the interactions of four different organic ligands with synthesized TiO₂ NPs in aquatic media have been investigated. Adsorption and aggregation interaction will be discussed in more detailed predominantly according to the results from paper I and II. Additionally a comparison between binary and ternary systems will be given with focus on the results obtained in paper III and IV. The following results will be discussed in more detail in this chapter:

- Aggregation behavior of TiO₂ NPs in aquatic environments
- Ligand adsorption onto TiO₂ NP surface; importance of molecular structure and environmental characteristics
- DLVO interaction energies of TiO₂ NPs with organic ligands
- Adsorption of 2,3-DHBA; a shift in color
- Metal ions and NPs and the formation of ternary surface complexes
- Time dependent study and the dynamic environment

4.1 AGGREGATION BEHAVIOUR OF TiO₂ NPS IN AQUATIC ENVIRONMENT

Environmental concerns of synthetic nanomaterials entering the environment has raised a lot of attention in recent years and several studies in this field have been performed. In previous studies by Baalousha et al.⁶⁸ and Domingos et al.⁹⁴ the aggregation of TiO₂ particles was studied and the effects of various concentrations of Suwannee River Fulvic Acid (SRFA), as well as pH and ionic strength were evaluated. For pH values close to the point of zero charge, aggregation was observed to increase and an increase in ionic strength generally resulted in increased aggregation independently of pH. Adsorption of SRFA was furthermore observed to result in less aggregation of TiO₂ NPs, presumably due to increased steric repulsion according to Domingos et al. (2009)⁹⁴. An important parameter missing in the above mentioned studies is the time dependence of aggregation.

In paper I, the initial aggregation during the first 15 minutes of reaction was investigated at pH 2.8. The main focus of the aggregation studies was to investigate the influence of the type and concentration of organic ligand on the colloidal stability of suspension over short time. Results showed that the hydrodynamic diameter changed with time and was dependent on the ligand concentration as well as particle concentration at pH 2.8 (Fig. 14). At this pH the bare particles are stable and are highly positively charged but when introducing a ligand to the suspension aggregation started to occur. Very different behavior in initial aggregation was observed and 2,3-DHBA and 1,2,4-BTCA gave rise to larger aggregates than phthalic acid did. Initial aggregation during the first 25 seconds in the TiO₂-SRFA system was relatively fast (Fig. 14d) and did not significantly change with time. Instead the system reached a semi-stable condition at which larger aggregates were formed with increased concentration of SRFA.

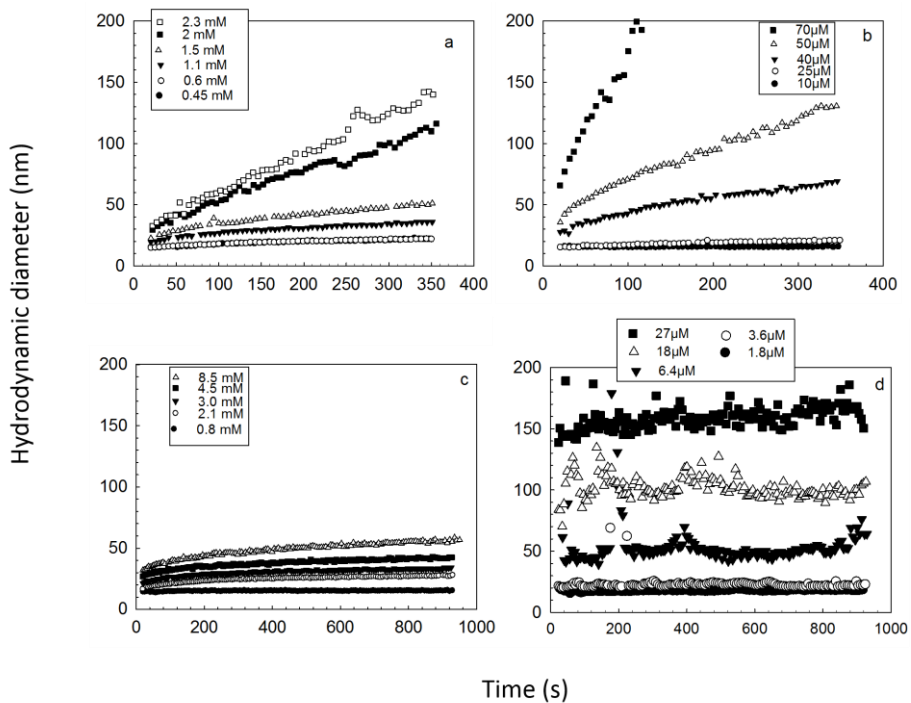


Figure 14 Hydrodynamic diameter after addition of a) 2,3-dihydroxybenzoic acid (2,3-DHBA), b) 1,2,4-benzenetricarboxylic acid (1,2,4-BTCA), c) phthalic acid, and d) Suwannee river fulvic acid (SRFA) respectively, as a function of time followed by DLS. Symbols represent concentrations of the respective organic molecule (From paper I)⁴

4.2 LIGAND ADSORPTION ONTO TiO₂ NP SURFACE; IMPORTANCE OF MOLECULAR STRUCTURE AND ENVIRONMENTAL CHARACTERISTICS

Adsorption of organic ligands on NPs is of high interest for the development of NP risk assessments, since the adsorption will alter the mobility of the particles and consequently their fate and bioavailability in the aquatic environment. Organic molecules adsorb to particle surfaces through electrostatic and/or specific interactions with particle surface sites, although hydrophobic interactions might also contribute to the adsorption of large macromolecules, such as NOM. NOM is found in most natural waters and sediments. Several studies have investigated the interactions of NOM, such as humic and fulvic substances, with particle surfaces with the aim of providing information about the fate and toxicity of NPs entering the environment.^{45, 46, 48, 99} However, only a few studies have investigated the effect of smaller organic molecules¹²² that may be found in natural systems, either naturally occurring or as byproducts through degradation of other substances. Additionally, it is important to know how different functional groups interact with particle surfaces. The particles used in this study have shown to be stable in size and charge at pH values less than 3. While introducing organic ligands to the particle suspension at pH 2.8 they start to interact with the surface. The adsorption of all four ligands investigated; 2,3-DHBA, 1,2,4-BTCA, phthalic acid and SRFA, was shown to be dependent upon ligand concentrations with more adsorption on the surface with increased concentrations (Fig 15). 1,2,4-BTCA did not show a significant change in adsorption when increasing the ligand concentration compared to the other ligands. Additionally, phthalic acid seemed to not immediately interact with the surface, since no phthalic acid was adsorbed after ten minutes on the rotator (day 0) (Fig. 15c). However, after 24 h mixing, a clear trend was observed with increased adsorption as the ligand concentration increased.

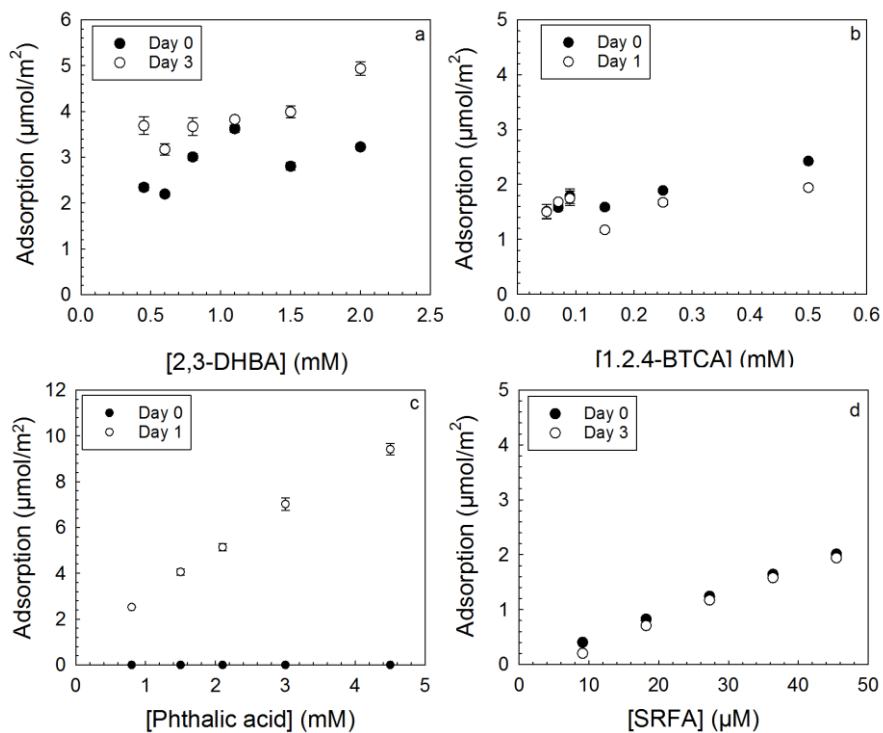


Figure 15 Adsorption of a) 2,3-DHBA, b) 1,2,4-BTCA, c) phthalic acid and d) SRFA on TiO_2 nanoparticles displayed as adsorption ($\mu\text{mol}/\text{m}^2$) as a function of initial total concentration of the respective organic molecule. Initial particle size = 13 nm; BET surface area = 206 m^2/g ; Solid conc = 104 mg/L. Error bars correspond to standard deviation of three replicates. (From paper I)⁴

In paper II, pH was increased to 5 and similar batch adsorption experiments were performed as in paper I, and results after 24 h mixing is presented in figure 16. Similar trends as in pH 2.8 were found, i.e. the amount of ligands adsorbed to the particle surface increased with increasing ligand concentrations. However, for 1,2,4-BTCA this effect was significantly more pronounced at pH 5 (Fig. 16b). Additionally, the adsorption of phthalic acid (Fig. 16c) showed a significantly higher adsorption maximum than for the other ligands, which indicated multilayer adsorption.

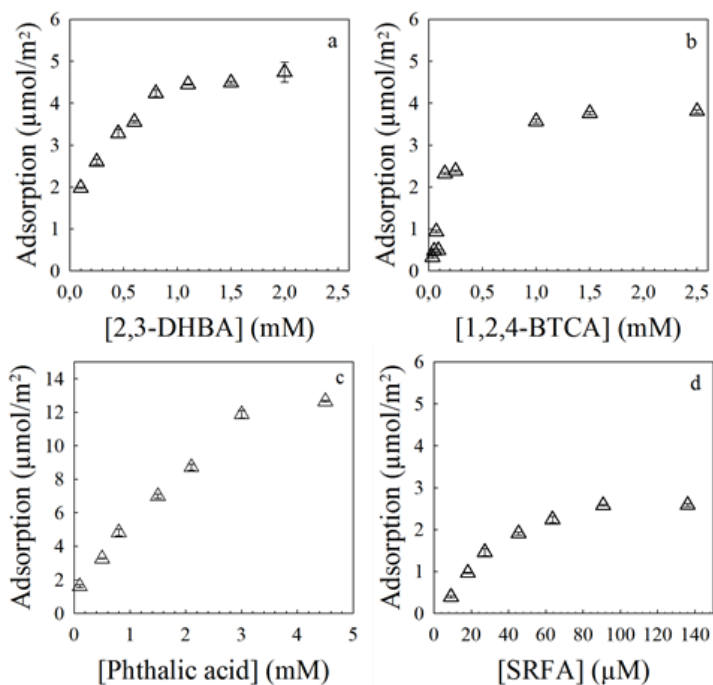


Figure 16 Adsorption of a) 2,3-DHBA, b) 1,2,4-BTCA c) phthalic acid, and d) SRFA on TiO₂ NP after 24 h mixing on rotator displayed as adsorption (μmol/m²) as a function of initial total concentration of the organic molecule. Initial particle size = 13 nm; BET surface area = 162 m²/g; Solid concentration = 100 mg/L. The error bars correspond to standard deviation of duplicates. Note the different scales on the axes. (From paper II)³

It was clear that the adsorption behavior varied significantly depending on the molecular structure of the ligand. These differences were elucidated with IR spectroscopy measurements, showing that the smaller molecules interacted differently with the TiO_2 surface by the formation of inner- and/or outer-sphere complexes depending on pH and type of functional groups. 1,2,4-BTCA with three carboxylic acids showed predominance of inner-sphere complexation at pH 2.8 and a chelate complex with two of the three carboxylic groups interacting with the surface, forming a mononuclear surface complex (Fig. 17f and 18a). When increasing the pH to 5 the adsorption was most probably driven by charge differences between the surface and the ligand and an outer sphere surface complex was formed (Fig. 17e and 18b).

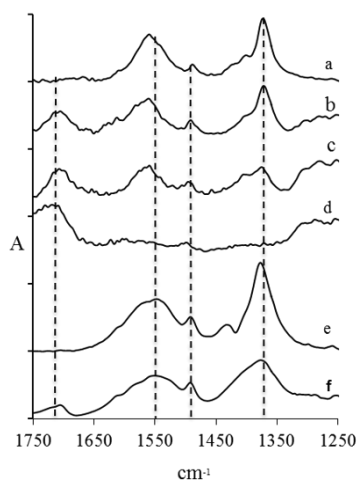


Figure 17 IR solution spectra of 1,2,4-BTCA as function of pH (a-d) and IR spectra of 1,2,4-BTCA adsorbed on TiO_2 surface (e and f). Solution spectra were collected at a ligand concentration of 10 mM at pH 10.8 (a), 4.5 (b), 3.0 (c) and 1.2 (d), while the spectra of adsorbed ligands were collected at pH 5 at ligand concentration of 4 mM (e) and pH 2.8 ligand concentration of 5.3 mM (f).

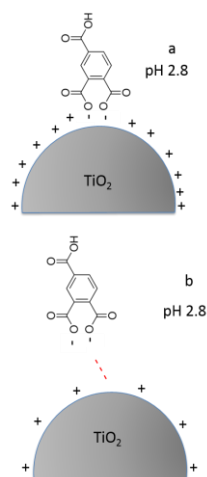


Figure 18 Illustration of possible complex formation according to IR spectroscopic study showing 1,2,4-BTCA inner sphere complex at pH 2.8 (a) and outer sphere at pH 5 (b)

The interaction of phthalic acid with the particle surface at pH 5 indicated the formation of an inner sphere chelate complex (Fig. 19) at low concentrations. With increased concentration, the IR spectra suggested the existence of a deprotonated outer sphere/hydrogen bonded species similar to the 1,2,4-BTCA complex at pH 5 (Fig. 20b). When further increasing the concentration of phthalic acid the existence of outer sphere complex was increased, while decreasing the pH to 2.8 only minor changes in the spectra were observed (Fig 20a).

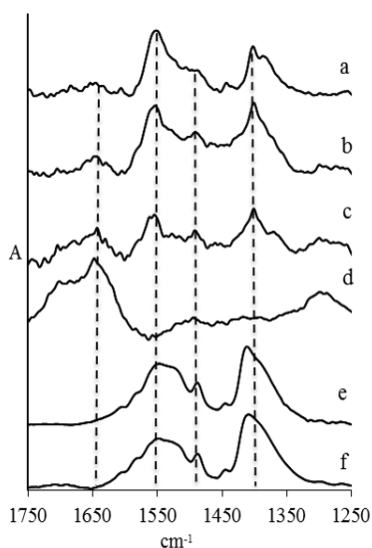


Figure 19 IR solution spectra of phthalic acid as function of pH (a-d) and IR spectra of phthalic acid adsorbed on TiO_2 surface (e and f). Solution spectra were collected at a ligand concentration of 10 mM at pH 10.7 (a), 4.5 (b), 3.0 (c) and 1.5 (d), while the spectra of adsorbed ligands were collected at ligand concentration of 6.25mM pH 5 (e) and pH 2.8 (f). From paper II³

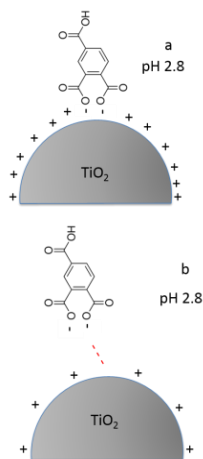


Figure 20 Illustrations of possible complex formation according to IR spectroscopic study of phthalic acid with formation of inner sphere complex with contribution of outer sphere complexes at pH 2.8

IR spectra of the 2,3-DHBA system showed significant differences between aqueous solution species compared to the ligand adsorbed to the particle surface (Fig. 21) and suggested oxidation of the hydroxyl groups. This was perhaps connected with ligand dimerization/polymerization that has been shown for catechol like molecules.^{123, 124} Additionally, very similar products at pH 5 and 2.8 were formed, as was indicated by the near identical IR spectra (Fig 21 c and d). These results indicated the importance of studying not only large macromolecules such as NOM but also smaller organic molecules in the presence of NPs.

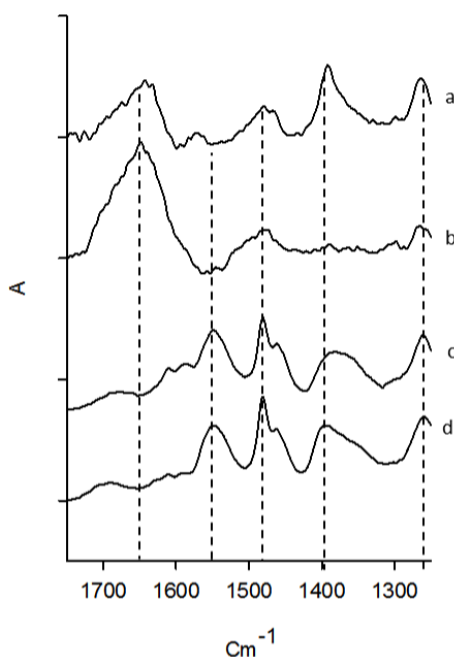


Figure 21 IR solution spectra of 2,3-DHBA as a function of pH (a and b) an IR spectra of DHBA adsorbed on the TiO_2 surface (c and d). Solution spectra were collected at ligand concentration of 10mM at pH 4.8 (a) and 1.5 (b), while the spectra of adsorbed ligands were collected at pH 5 (c) and pH 2.8 (f). From paper II³

4.3 DLVO INTERACTION ENERGIES OF TiO₂ NPS WITH ORGANIC LIGANDS

In this thesis a classical DLVO model was used and interaction energies between TiO₂ and the four different organic ligands are presented in figure 22. Experimental values of ζ -potentials and particle sizes were used in the calculations. In the 2,3-DHBA-TiO₂ system the DLVO interaction energies showed that Van der Waals attractive forces were dominating at all concentrations investigated at pH 5 (Fig. 22a and b), while EDL repulsive forces were dominating for ligand concentrations ≤ 0.25 mM at pH 2.8.

In the 1,2,4-BTCA-TiO₂ system the DLVO calculations showed that the EDL repulsive forces were very small and Van der Waals attractive forces were dominating at all concentrations investigated at pH 5 (fig. 22d) and decreased with increased concentration. When decreasing pH to 2.8 (Fig. 22f) almost opposite behaviors were observed where high concentration of the ligand was contributing to destabilization of the particles. Phthalic acid showed similar behavior as 1,2,4-BTCA with higher energy barrier at pH 2.8 compared to pH 5 (Fig. 22g-i). DLVO interaction energies between TiO₂ particles and SRFA are shown in Fig. 22 j-l. At day 0 (sampling after 15 minutes mixing on the rotator) in pH 5 (Fig. 22j), the attractive forces were relatively small for concentrations ≥ 45 μ M of SRFA, and EDL repulsive forces were dominating thus stabilized the system. In pH 2.8 increased concentration of SRFA gave rise to a less stable system (Fig. 22k). The DLVO model used in this study presumes small spherical particles. However, according to the DLS measurements the TiO₂ particles aggregated when interacting with the ligands and the particles were most likely not spherical. Despite the non-spherical shape, these results have contributed to the understanding of what type of interactions occurred between the TiO₂ particles and the ligands.

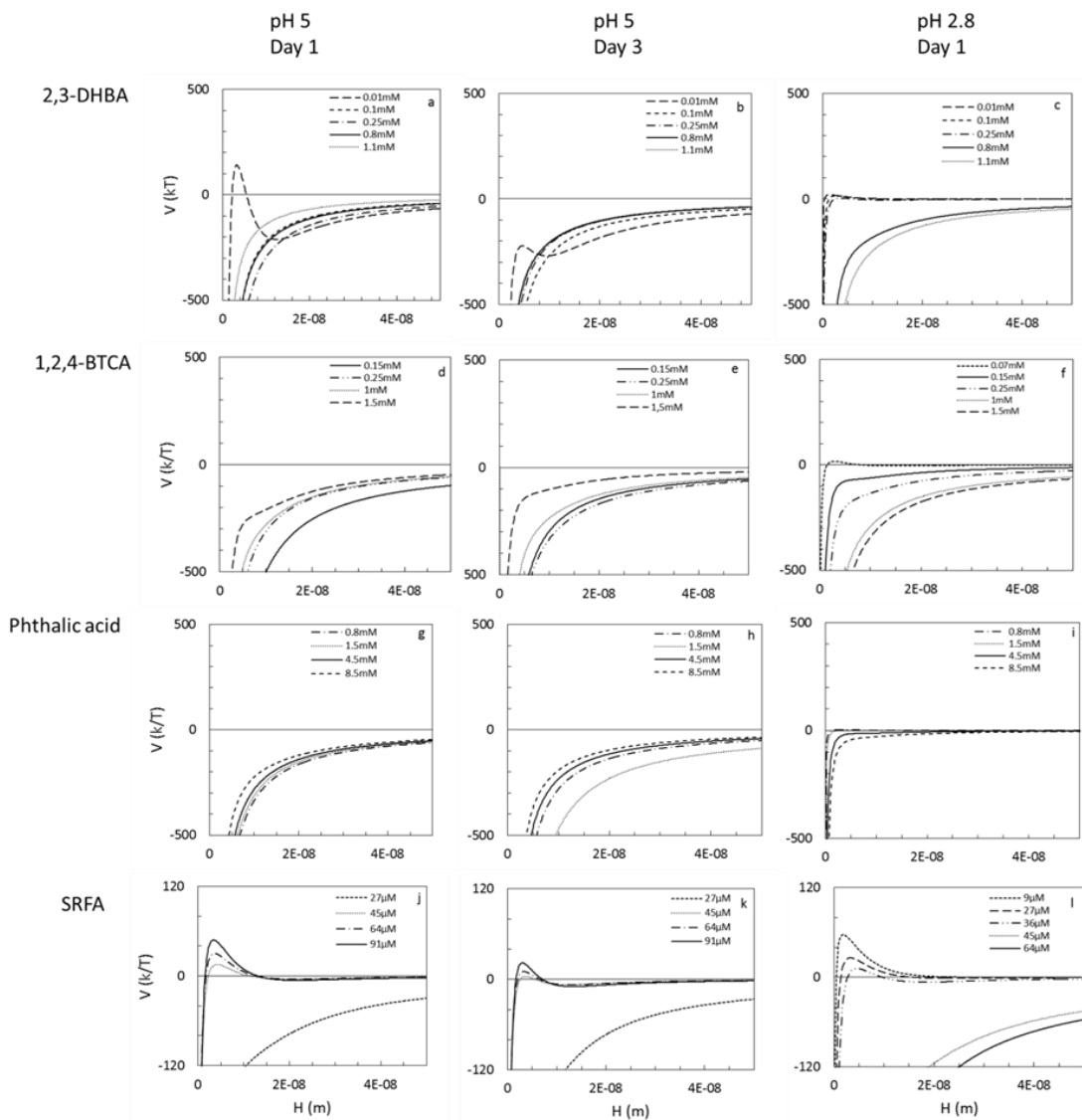


Figure 22 DLVO interaction energies between TiO_2 particles and 2,3-DHBA (a-c), 2,3-1,2,4-BTCA (d-f), phthalic acid (g-i) and SRFA(j-l). From paper II³

4.4 METAL IONS AND NANOPARTICLES AND THE FORMATION OF TERNARY SURFACE COMPLEXES

In natural waters not only organic material may interact with NPs. Other species such as inorganic molecules, salts and metal ions present may also adsorb and modify the surface, thus can affect the fate and transport of NPs. The presence of heavy metal contaminants in soil and natural waters has been a matter of concern for several years since it has a negative effect on the environment.¹²⁵ It is important to remediate the contaminated water to minimize this negative effect. Adsorption of heavy metal onto mineral surfaces has been used to clean these contaminated waters. Nanotechnology has been developed in this field and the use of NPs has increased due to their high surface area and the capacity to adsorb molecules and metal ions.¹²⁶⁻¹²⁸ However, the efficiency of heavy metal removal by NPs may be affected negatively due to shifts in pH and adsorption of organic ligands present in the water column, since both pH and organic ligands may influence metal speciation and thus their adsorption. Additionally, organic ligands may form complexes with metal ions in the water, which affects their adsorption behavior. This will in turn affect the colloidal stability of NPs released into the environment. In paper III and IV the interactions of 2,3-DHBA (Paper III) and SRFA (Paper IV) respectively, with TiO₂ NPs in the presence of Zn²⁺ ions were investigated.

In addition to the experimental study, molecular dynamics (MD) simulations were performed to get better insight into the complexation of the organic ligands with Zn²⁺ in aqueous solution. Deprotonated 2,3-DHBA molecules in water showed the tendency of pi-stacking which most probably was due to attractive interactions between aromatic rings (Fig. 23a). For protonated 2,3-DHBA, this effect was not as pronounced, probably due to repulsive electrostatic interactions contributed from the negatively carboxylic groups. Deprotonated 2,3-DHBA showed possible complexation with Zn²⁺ (Fig.23b), while the protonated did not. MD calculations also showed complexation between SRFA and Zn²⁺ (Fig. 23c) depending on pH in solution and Zn²⁺ interacted stronger with increasing deprotonation state of SRFA.

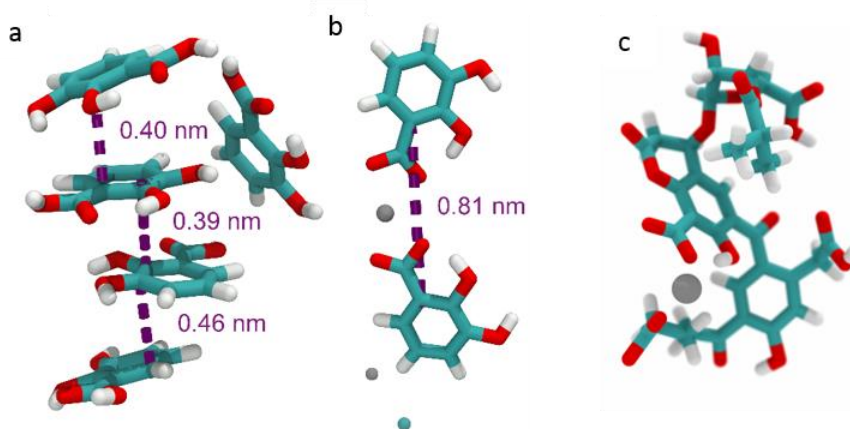


Figure 23 Snapshots from MD simulations present interactions between (a) DHBA molecules in water and (b) DHBA- molecules in 0.5M ZnCl₂ and (c) complex of SRFA²⁻ with Zn²⁺. Modified from paper 3 and 4.

The experimental study showed that the effect of Zn²⁺ on the colloidal stability was more pronounced at pH 5 compared to pH 2.8 in both systems investigated. Depending on concentration, ligand adsorption induced charge inversion, i.e. ζ -potential was negative at pH 5 (Fig. 24). However, when Zn²⁺ was present the charge turned less negative, indicating adsorption of Zn²⁺ to the particle, which also was seen in the adsorption study where more Zn²⁺ was adsorbed with increased concentration. Adsorption of both the ligands and Zn²⁺ varied depending on the concentration of Zn²⁺ and in both systems the experimental data showed strong evidence of the formation of ternary surface complexes.

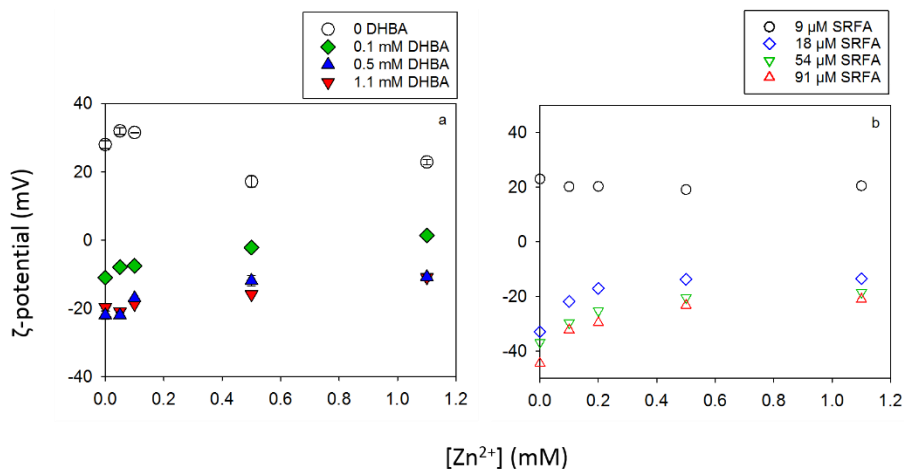


Figure 24 ζ -potentials of TiO_2 nanoparticles as a function of Zn^{2+} concentration, and in the presence of 2,3-DHBA(a) and SRFA (b) at pH 5. Figure modified from paper 3 and 4.

The presence of Zn^{2+} also affected the size of the particles. In the TiO_2 -DHBA-Zn system, the aggregation study showed increased aggregation with Zn^{2+} concentration at the highest ligand concentration tested, which might be due to enhanced screening of the particles. Also, as was seen in the MD calculations (Fig. 23b), complexation between Zn^{2+} and 2,3-DHBA in solution may affect the interaction with the TiO_2 surfaces, with the formation of larger aggregates. In the TiO_2 -SRFA-Zn system at pH 5, formation of larger aggregates with increased concentration of Zn^{2+} was observed. This effect in combination with the decreased negative charge, was probably due to the deprotonation of the SRFA molecule which was supported by the DFT calculations (Table 1). If large aggregates are formed there is a potential risk that the particles will sediment in the water column and be buried in the sediment, thus becoming bioavailable to organisms living in the sediment. Also, the bioavailability of essential metals and organic ligands in the water column may be decreased, in turn affecting the organisms living in this biota. There are several different scenarios that may have a negative effect on the environment even though it may not seem to have acute toxicity. It is therefore of high importance to further investigate both binary and ternary systems to get a better understanding of the mechanisms behind the aggregation and adsorption behavior of NPs in the environment.

4.5 ADSORPTION OF 2,3-DHBA, A SHIFT IN COLOR OBSERVATION

In this thesis, the interactions of 2,3-DHBA with TiO_2 NPs in terms of aggregation, charge and adsorption mechanisms have been thoroughly investigated. An interesting observation was that with the addition of TiO_2 particles to the 2,3-DHBA solution, the transparent solution turned into a slightly yellow color after addition of the particles and the color got more intense as the concentration of DHBA was increased (Fig. 25).

Similar observation was not seen for the other smaller molecules (phthalic acid and 1,2,4-BTCA). Since those molecules only have carboxylic functional groups, the shift in color indicated that the OH-functional groups of 2,3-DHBA were somewhat involved in the interactions with the TiO_2 surface, which was also the interpretation of the long-term study presented in paper I. Moreover, the yellow color at pH 2.8 was more distinct compared to pH 5 which might be an effect of particle size. At pH 2.8 the particles were ~ 13 nm in diameter compared to ~ 1100 nm at pH 5. When the size is increased, the specific surface area is decreased, which affects the interaction energy.

To verify the mechanisms behind the shifts in color, an additional study needs to be conducted, which was not within the scope of this thesis. Nonetheless, these are valuable observations since they partly support the experimental results; i.e., time in suspension affected the reaction behavior (as was discussed in section 4.3), with the change in color being more pronounced after 48 h.

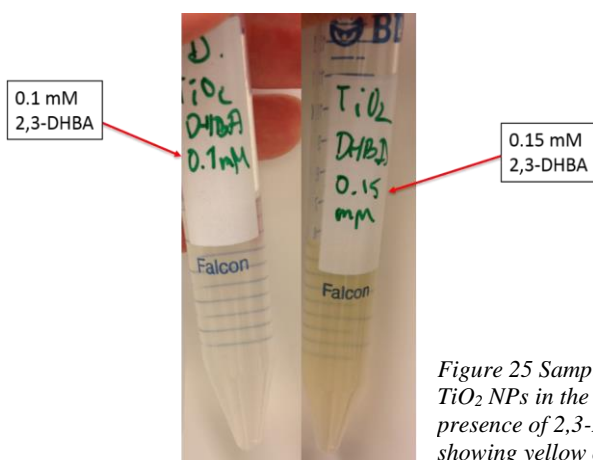


Figure 25 Samples of TiO_2 NPs in the presence of 2,3-DHBA showing yellow color

4.6 TIME STUDY AND THE DYNAMIC ENVIRONMENT

In paper I, the long-term effect of the interactions between 2,3-DHBA and SRFA, respectively, on TiO_2 particles was investigated by following the size and charge over a time-period of up to 9 months. In the natural environment constant changes occur that may affect the colloidal stability of the particles, such as change in temperature caused by seasonal variations, differences in ionic strength and also concentration and the presence of different organic and inorganic species. What happens if these parameters are set to be constant in for instance a water column; will the colloidal stability be affected over time anyway? This was one of the questions that arose during the long-term study in paper I. As mentioned earlier, samples were kept on a rotator to ensure mixing and in some way mimic turbidity in natural waters and avoid sedimentation. Results from paper 1 showed that both charge (Fig. 25) and size were changing significantly with time in the TiO_2 -2,3-DHBA system. A stabilization effect was also observed at certain concentrations. Interestingly, SRFA did not show the same behavior and it seemed likely that the TiO_2 -SRFA system reached a steady state faster.

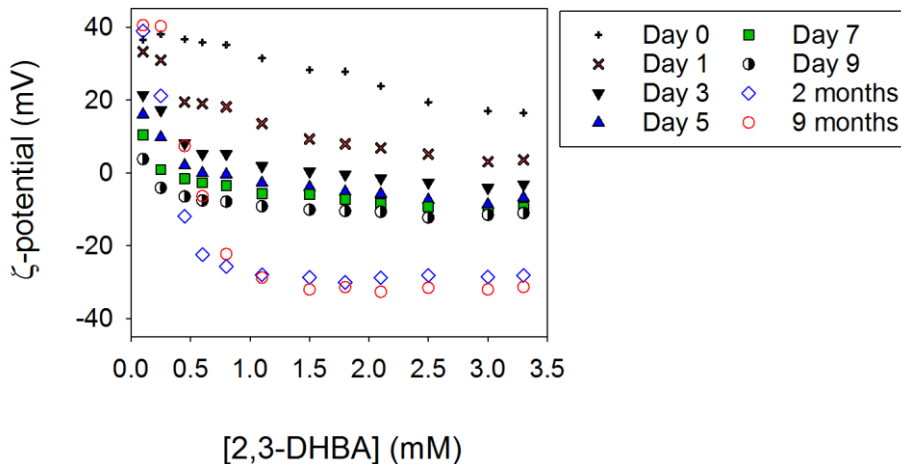


Figure 26 ζ -potential and hydrodynamic diameter of TiO_2 nanoparticles over time and at different total concentrations of 2,3-dihydroxybenzoic acid (2,3DHBA). pH was constant at 2.8 and particle concentration was 0.1 mg/L. Symbols represent time that passed since the start of the experiment. Figure modified from paper I⁴

In paper II, a kinetic study of all four systems was performed where adsorption, ζ -potential and size were measured up to three months and results are presented in figure 26. The 2,3-DHBA- TiO_2 system (Fig. 26a-c) showed decreased size, increased negative charge and increased adsorption with time. This indicated that 2,3-DHBA had a certain stabilization effect on the TiO_2 particles over time depending on ligand concentration.

In the 1,2,4-BTCA- TiO_2 system (Fig. 26d-f), very large aggregates (2500-5000 nm) were formed at day 1 with a decrease in size with time, while ζ -potentials and adsorption data showed no significant change during the time period of 23 days. Interaction of phthalic acid with TiO_2 NPs showed only small variations during 14 days of measurements. ζ -potentials were very close to zero and aggregate sizes approx. 2000-3000 nm (Fig. 26g-i). As for phthalic acid, SRFA showed only minor changes with time. Sizes, ζ -potentials and adsorption varied with concentration, but not with time.

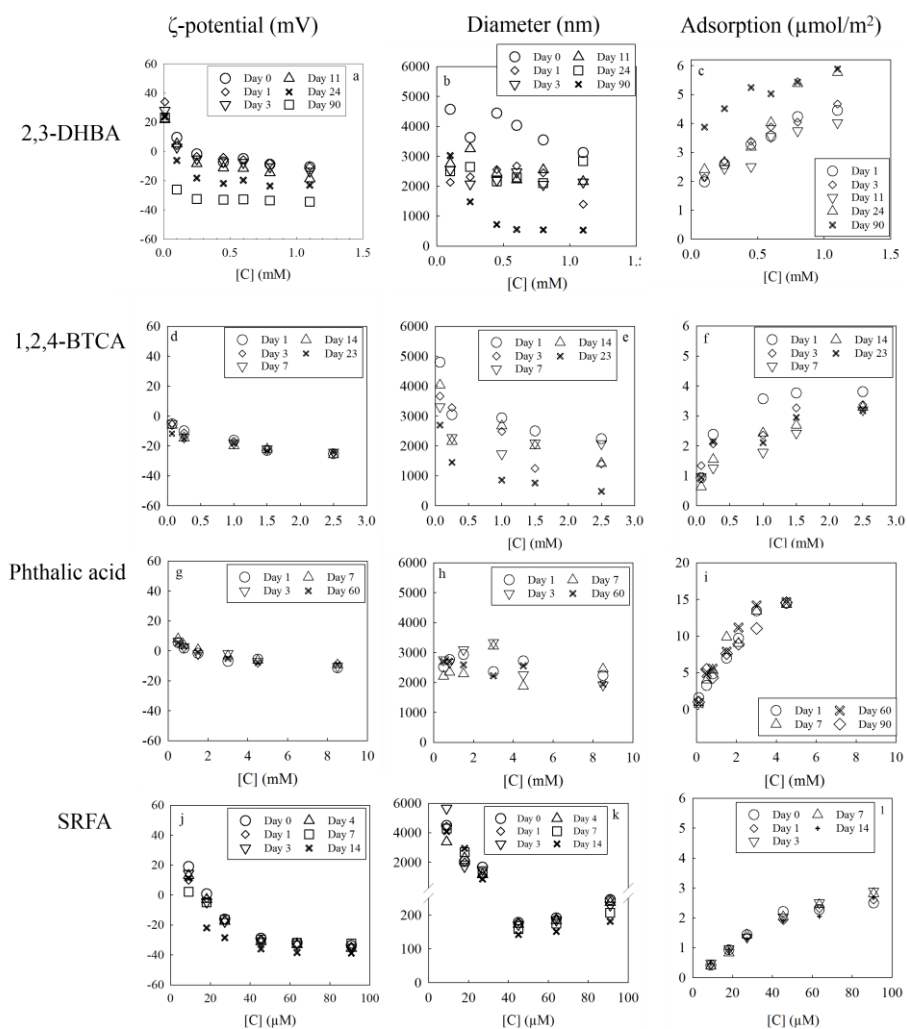


Figure 27 ζ -potential; d_H and adsorption of TiO_2 nanoparticles over time and at different total concentrations of 2,3-DHBA (a-c), 1,2,4-BTCA (d-f), Phthalic acid (g-i), and SRFA (j-l). pH was constant at 5 ± 0.1 and particle concentration was 100 mg/L . (Figure from paper II)³

These results indicated that the interactions between particles and ligands (or other molecules) are highly dependent upon ligand concentration and functional groups. It is interesting to note that 2,3-DHBA interactions with the TiO_2 particles seemed to be the most affected by time, and the question is “why is it so”? According to a theoretical study by Redfern et al,¹²⁹ possible interaction of catechols with TiO_2 NPs (anatase) may

form monodentate or bidentate bonding with the OH-groups attached to the particle surface. Additionally, the dimerization process suggested in the IR spectroscopic study in paper II may cause a shift in the pK_a due to polarization of the OH-group making deprotonation of the COOH-group occur to a larger extent, which in turn may explain the decreasing ζ -potential values. Another explanation is that due to incomplete surface coverage, a rearrangement of surface complexes occurred as the system tried to reach equilibrium, which obviously takes time, indicating a dynamic system. These observations point out the need for more studies in this field over long time periods and perhaps also include seasonal variation parameters such as light and temperature.

5 CONCLUDING REMARKS

Results in this thesis present the importance of studying interaction processes between NPs and ligands at a molecular level in order to get a full understanding of the mechanisms behind NP stability. Several interesting implications of TiO₂ (anatase) NP aggregation were observed and the colloidal stability of TiO₂ NPs was highly influenced by the nature of organic ligands. TiO₂ NPs interacted differently with the ligands depending on ligand concentration, type of functional groups, pH, and, in some cases, time in suspension. This was supported by IR spectroscopic data showing that the ligands interacted with the TiO₂ particles in different ways, i.e. through inner sphere and outer sphere complex formation. It was shown that phthalic acid formed inner sphere complexes at the TiO₂ surface with contribution of outer sphere complexation at higher ligand concentrations at pH 5. 1,2,4-BTCA with one additional carboxylic group compared to phthalic acid, showed the formation of inner sphere chelating complex at pH 2.8 while at pH 5, an outer sphere complex was formed. Additionally, 2,3-DHBA underwent a dimerization/polymerization upon interaction with the TiO₂ surface. Complexation of Zn²⁺ with 2,3-DHBA and SRFA, respectively, affected the colloidal stability of TiO₂ NPs by interacting with the surface to form larger aggregates with varying ζ -potentials. The combination of molecular dynamic simulations and experimental aggregation and adsorption data gave valuable information to better understand the colloidal stability of TiO₂ NPs in the presence of both organic ligands and metal ions. These results enhance the importance of studying ternary systems in order to better relate to natural conditions.

Results will provide new and valuable information to better determine the fate of TiO₂ NPs in natural waters. Understanding the adsorption and aggregation behavior is important in order to understand the fate, transport and bioavailability of not only the particles but also organic molecules and metal ions associated with the particles.

Results showed that time in suspension affected the interaction processes in the different particle-ligand systems, which emphasizes the need for kinetic studies over long time periods in order to get a better understanding of the fate and behavior of synthetic nanoparticles in aquatic environments. The

present work makes a significant contribution to the general understanding of particle-ligand interactions over longer time periods (weeks and months), which is required to understand, describe and predict natural processes involving metal oxide nanoparticles in ecosystems that are very dynamic.

With the increased use of synthetic TiO₂ NPs in several applications, such as sunscreens and paints, the potential release into the environment is suggested to increase. Results presented in this study should be considered as an important piece of information to be combined with data from systems including NOM, metals and inorganic particles among others, in order to increase certainty in risk assessments of synthetic NPs in natural waters.

Additionally, results might be applied to other similar systems containing organic ligands, such as pharmaceuticals present in natural waters that may interact with particle surfaces. For instance, 2,3-DHBA is a by-product from aspirin metabolism while phthalic acid is derived from benzene used in pharmaceutical production and are excreted through urine where they may end up in natural waters and attach to particles present in the water. This will alter the colloidal stability of the particles and affect the exposure of NPs in both water and sediment.

6 FUTURE PERSPECTIVES

Although new valuable information has been obtained through this thesis work regarding TiO₂ nanoparticle stability, more information and more studies need to be performed in order to make qualified and reliable risk assessments concerning NPs released into the environment. There are especially a few future studies that I would like to address.

In this thesis the adsorption behavior of different molecules to the TiO₂ surface have been thoroughly investigated. However, *desorption* mechanisms have not been investigated and this could be an important factor when determining the colloidal stability of particles in suspension. We have demonstrated that depending on pH and the molecular structure of the ligand, inner and or outer-sphere complexes are formed. Inner sphere complex formation involves chemical bonds, while outer sphere complexation is more electrostatically driven. These differences in interaction modes make them more or less probable to detach from the surface and be released into the bulk. This may cause the particles to disaggregate and remain in the water column instead of sedimenting out of the water. This changes the bioavailability of not only the particles but also natural organic matter present in the water.¹³⁰

Analytical restrictions is another variable that may be improved to get more information about the shape and structure of the particles and aggregates. In paper I, we have used TEM to reveal this information but the sample preparation was very difficult since the sample must be completely dry and the drying process might cause changes in the crystal structures. If instead CRYO-EM would have been used maybe structural information could have been achieved. In CRYO-EM the liquid sample is frozen quickly and the analyzed sample is assumed to be intact and not have the time to crystallize.

In paper II, we used simple DLVO calculations to obtain information about the interaction energies but there are also several *non-DLVO forces*, such as steric interactions and hydration forces that may influence the stability of NPs in aqueous suspensions¹³¹. By using the analytical models which include non-DLVO interactions, more information about the specific interaction energies would be achieved but at the same time more elaborate studies to find reasonable parameter values are required. As mentioned throughout this thesis,

particles may adsorb natural organic matter (NOM) that is known to stabilize colloids. Information of steric interactions through non-DLVO calculations is therefore important in order to determine fate of NPs in aquatic environments.

ACKNOWLEDGEMENTS

Have you heard about nanoparticles? That was one of the questions I got at the interview for the position as a PhD student. My quick response was yes, which was true, but the fact was that I didn't know much about nanoparticles at all, and I sure did not know their wide applications and use in different consumer products. I started my chemistry career as an analytical chemist at a large pharmaceutical company in Sweden, so this was a complete new area for me which on the other hand was one of the challenges that brought me to actually say yes to the position, a decision which I never regretted. Who said it was going to be easy? There are several people who helped me and supported me during this period to whom I would like to acknowledge:

My supervisor **Caroline Jonsson**, a simple thank you is not enough. I am so grateful for you giving me the opportunity to do this journey and supervising me. I am just sorry you couldn't be here to the bitter end. You have always encourage me and never ever stopped believing in me. Through good times and bad, almost like a marriage. I could never have done this without you, so a big huge enormous thank you! I wish you the best of luck and I hope we will have more interesting discussions as "snillen spekulerar".

My supervisor **Zareen Abbas**, for all your patience, guidance and help during my p.H.D, you have supported me in the best possible way to make this thesis come to a closure and I am so grateful for that. Thank you Zareen!

Johan Bergenholtz, thank you for all help and guidance with the light scattering instrument and for your always positive and helpful attitude. Your enthusiasm about science have been an inspiration.

My examiner **Stefan Hulth**, it hasn't always been easy, your positive attitude and support have been priceless. I will always remember your signpost above your door. Your door was always open and one could not feel anything else than welcome. Thank you!

Julian Gallego-Urrea, what would I have done without you? You gave me time and a big piece of your knowledge. Thank you for your enormous patience with me and for providing me with candy once and a while when I needed it the most.

Per Persson for giving me the opportunity to measure and learn about IR spectroscopy and for all the help with the interpretation of results, I would n't have done it without you.

Kristina Hedfalk, for letting me use the ultracentrifuge during the years I really appreciated it. Also for time spent during “lunch-running” all though my participation was not as high in the forest as in the room of centrifugations.

Krzysztof Kolman for giving me the chance to learn more about the world of simulations. Thank you for all support and a great collaboration.

Co-authors **Jörgen Rosenqvist**, **Martin Hassellöv** and **Stefan Gustafsson** thank you for all scientific discussions and the contributions to the papers. And Jörgen for providing me with emergency supplies once and a while.

András Gorzsás for introducing me to IR spectroscopy, for the help, support and guidance during measurements. All though it did not work out as planned (but what does?), it was a very good experience and I learned a lot.

Lennart Sjölin for all support in teaching duties. Thank you for giving me the opportunity to work with you in the “upptäckarklubben”, it was a privilege. And thank you for the company and nice discussions in the lunch room, mostly about skiing☺

Jenny Perez Holmberg, my roomie, who not only introduced me to the synthesis of TiO₂ nanoparticles but for introducing “emergency supplies”, how could one survive without it?

Jenny Bergman, always supporting and thank you for your shoulder to cry on when needed. But most for all thank you for times of laughter’s, discussions and company in the coffee room.

Jeanette Ulama, thank you for every moment we shared and the laughter’s, it is always fun to be around you. For very early notice my need for food and for provision when needed, Karin with an empty stomach is no good combination☺

Stina Lindqvist, you were gone and you came back. I simply say thank you!

Kristin Jonsson and others on 5th floor, thank you for the coffee and always welcoming attitude, it’s been a pleasure.

Thank you all **colleagues** on fourth floor for every discussions in the lunch room and for letting me taste candy with flavors from all around the world!

People at the administration, for your positive attitude and patience when learning how to write a travel expense claim correctly, it took me about 4 years to learn.

The **group of marine science** for help and guiding whenever question arise and for all chats and laughter's. You left an empty whole after leaving the building.

My parents, **mamma Ulla** and **pappa Janne** for supporting me and taking care of my children when ever needed, I wouldn't be able to do this without your help.

My always happy sister **Eva** for letting me be me and providing with a "second home" in Åre, Mountains, snow and a pair of skis and I am in heaven and of course in the best company with you and your boys. And my brother **Per** for all good advice during the way and (when there was time), fun and energetic vacation trips. It is more fun to be around you now than when we were kids☺

Alexander, for giving me positive energy and providing me with food when working late hours, I can't thank you enough. You have lots of dinners to look forward to and I promise you it will not only be candy and a bag of crisps but maybe not "vita dukar". Also, I will offer with great company, perhaps the best☺

And last but not least I would like to thank my children, **Kerstin** and **Lottie**, for giving me energy when I needed it the most. Thank you for having the patience with a stressed mother (not seldom I wondered who is the parent and who is the child). Jag älskar er till rymden och tillbaka. Ni är bäst!

Family and friends, you know who you are☺

And to those who are not with us anymore, you are missed.

The research in this thesis was funded by The Swedish Research Council - Vetenskapsrådet and The Hasselblad Foundation.

REFERENCES

1. W. Stumm, in *Aquatic Chemistry*, American Chemical Society, 1995, vol. 244, ch. 1, pp. 1-32.
2. M. Kaszuba, J. Corbett, F. M. Watson and A. Jones, *Philosophical transactions. Series A, Mathematical, physical, and engineering sciences*, 2010, **368**, 4439-4451.
3. K. Danielsson, P. Persson, J. A. Gallego-Urrea, Z. Abbas, J. Rosenqvist and C. M. Jonsson, *NanoImpact*, 2018, **10**, 177-187.
4. K. Danielsson, J. A. Gallego-Urrea, M. Hasselov, S. Gustafsson and C. M. Jonsson, *Journal of Nanoparticle Research*, 2017, **19**, 133.
5. R. P. Feynman, *Engineering and Science*, 1960, **23**, 22-36.
6. P. Iqbal, J. A. Preece and P. M. Mendes, in *Supramolecular Chemistry: From Molecules to Nanomaterials*, 2012, DOI: doi:10.1002/9780470661345.smc195.
7. H. Rohrer, *Proceedings of the National Academy of Sciences*, 1987, **84**, 4666-4666.
8. E. Ruska, *Bioscience Reports*, 1987, **7**, 607-629.
9. G. Binnig, C. F. Quate and C. Gerber, *Physical Review Letters*, 1986, **56**, 930-933.
10. M. Auffan, J. Rose, J.-Y. Bottero, G. V. Lowry, J.-P. Jolivet and M. R. Wiesner, *Nature nanotechnology*, 2009, **4**, 634.
11. E. Bekyarova, Y. Ni, E. B. Malarkey, V. Montana, J. L. McWilliams, R. C. Haddon and V. Parpura, *Journal of biomedical nanotechnology*, 2005, **1**, 3-17.
12. M. S. Dresselhaus, G. Dresselhaus and R. Saito, *Carbon*, 1995, **33**, 883-891.
13. A. Astefanei, O. Núñez and M. T. Galceran, *Analytica Chimica Acta*, 2015, **882**, 1-21.
14. B. S. Harrison and A. Atala, *Biomaterials*, 2007, **28**, 344-353.
15. A. Kiani, M. Rahmani, S. Manickam and B. Tan, *Journal of Nanomaterials*, 2014, **2014**, 2.

16. M. Bangal, S. Ashtaputre, S. Marathe, A. Ethiraj, N. Hebalkar, S. W. Gosavi, J. Urban and S. K. Kulkarni, *Hyperfine Interactions*, 2005, **160**, 81-94.
17. S. A. Corr, in *Nanoscience: Volume 1: Nanostructures through Chemistry*, The Royal Society of Chemistry, 2013, vol. 1, pp. 180-207.
18. E. Roduner, *Chemical Society Reviews*, 2006, **35**, 583-592.
19. J. Biener, A. Wittstock, T. F. Baumann, J. Weissmüller, M. Bäumer and A. V. Hamza, *Materials*, 2009, **2**, 2404-2428.
20. K. H. F. and W. Peter, *Angewandte Chemie International Edition*, 2011, **50**, 1260-1278.
21. V. H. Grassian, *The Journal of Physical Chemistry C*, 2008, **112**, 18303-18313.
22. Y. Volokitin, J. Sinzig, L. J. de Jongh, G. Schmid, M. N. Vargaftik and I. I. Moiseevi, *Nature*, 1996, **384**, 621.
23. M.-C. Daniel and D. Astruc, *Chemical Reviews*, 2004, **104**, 293-346.
24. J. Zheng, C. Zhou, M. Yu and J. Liu, *Nanoscale*, 2012, **4**, 4073-4083.
25. T. Ling, W. Qingshan, W. Alexander and C. Ji-Xin, *Photochemistry and Photobiology*, 2009, **85**, 21-32.
26. Y. Xu and D. Zhao, *Water research*, 2007, **41**, 2101-2108.
27. W.-x. Zhang, *Journal of Nanoparticle Research*, 2003, **5**, 323-332.
28. S. R. Kanel, J.-M. Grenèche and H. Choi, *Environmental Science & Technology*, 2006, **40**, 2045-2050.
29. K. V. Wong, N. Perilla and A. Paddon, *Journal of Energy Resources Technology*, 2013, **136**, 014001-014001-014009.
30. J. Lu, Z. Chen, Z. Ma, F. Pan, L. A. Curtiss and K. Amine, *Nature nanotechnology*, 2016, **11**, 1031.
31. V. L. Colvin, *Nat Biotech*, 2003, **21**, 1166-1170.
32. M. V. D. Z. Park, A. M. Neigh, J. P. Vermeulen, L. J. J. de la Fonteyne, H. W. Verharen, J. J. Briedé, H. van Loveren and W. H. de Jong, *Biomaterials*, 2011, **32**, 9810-9817.
33. A. Elsaesser and C. V. Howard, *Advanced drug delivery reviews*, 2012, **64**, 129-137.
34. M. R. Wiesner, G. V. Lowry, P. Alvarez, D. Dionysiou and P. Biswas, *Environ Sci Technol*, 2006, **40**, 4336-4345.
35. D. Lin, J. Ji, Z. Long, K. Yang and F. Wu, *Water research*, 2012, **46**, 4477-4487.

36. J. S. Bozich, S. E. Lohse, M. D. Torelli, C. J. Murphy, R. J. Hamers and R. D. Klaper, *Environmental Science: Nano*, 2014, **1**, 260-270.
37. A. J. Kennedy, H. M. S., S. J. A., D. K. M., C. M. A., G. J. C. and C. A. Weiss, *Environmental Toxicology and Chemistry*, 2008, **27**, 1932-1941.
38. A. E. Nel, L. Mädler, D. Velegol, T. Xia, E. M. V. Hoek, P. Somasundaran, F. Klaessig, V. Castranova and M. Thompson, *Nature materials*, 2009, **8**, 543.
39. P. J. Vikesland, R. L. Rebodos, J. Y. Bottero, J. Rose and A. Masion, *Environmental Science: Nano*, 2016, **3**, 567-577.
40. B. Nowack and T. D. Bucheli, *Environmental pollution*, 2007, **150**, 5-22.
41. Q. J. T.K., S. M. Cohen, W. Marja, P. Willie, H. A. Jan and v. d. M. Dik, *Environmental Toxicology and Chemistry*, 2012, **31**, 1019-1022.
42. J. Lee, S. L. Bartelt-Hunt, Y. Li and E. J. Gilrein, *Chemosphere*, 2016, **154**, 187-193.
43. R. A. French, A. R. Jacobson, B. Kim, S. L. Isley, R. L. Penn and P. C. Baveye, *Environmental Science & Technology*, 2009, **43**, 1354-1359.
44. R. Molina, Y. Al-Salama, K. Jurkschat, P. J. Dobson and I. P. Thompson, *Chemosphere*, 2011, **83**, 545-551.
45. J. A. Gallego-Urrea, J. Perez Holmberg and M. Hasselov, *Environmental Science: Nano*, 2014, **1**, 181-189.
46. M. Erhayem and M. Sohn, *Science of The Total Environment*, 2014, **468-469**, 249-257.
47. I. L. Gunsolus, M. P. S. Mousavi, K. Hussein, P. Bühlmann and C. L. Haynes, *Environmental science & technology*, 2015, **49**, 8078-8086.
48. B. J. R. Thio, D. Zhou and A. A. Keller, *Journal of Hazardous Materials*, 2011, **189**, 556-563.
49. R. Jain, N. Jordan, D. Schild, E. D. van Hullebusch, S. Weiss, C. Franzen, F. Farges, R. Hübner and P. N. L. Lens, *Chemical Engineering Journal*, 2015, **260**, 855-863.
50. S. Li and W. Sun, *Journal of Hazardous Materials*, 2011, **197**, 70-79.
51. V. Srivastava, D. Gusain and Y. C. Sharma, *Ceramics International*, 2013, **39**, 9803-9808.
52. J. W. Rasmussen, E. Martinez, P. Louka and D. G. Wingett, *Expert Opinion on Drug Delivery*, 2010, **7**, 1063-1077.

53. P. Falcaro, R. Ricco, A. Yazdi, I. Imaz, S. Furukawa, D. Maspoeh, R. Ameloot, J. D. Evans and C. J. Doonan, *Coordination Chemistry Reviews*, 2016, **307**, 237-254.
54. W. Wu, C. Z. Jiang and V. A. L. Roy, *Nanoscale*, 2016, **8**, 19421-19474.
55. J.-P. Jolivet, S. Cassaignon, C. Chanéac, D. Chiche, O. Durupthy and D. Portehault, *Comptes Rendus Chimie*, 2010, **13**, 40-51.
56. K. Becker, S. Schroecksnadel, S. Geisler, M. Carriere, J. M. Gostner, H. Schennach, N. Herlin and D. Fuchs, *Food and Chemical Toxicology*, 2014, **65**, 63-69.
57. K. E. Engates and H. J. Shipley, *Environmental Science and Pollution Research*, 2011, **18**, 386-395.
58. L. Fu, M. Hamzeh, S. Dodard, Y. H. Zhao and G. I. Sunahara, *Environmental Toxicology and Pharmacology*, 2015, **39**, 1074-1080.
59. G. Mattioli, A. Amore Bonapasta, D. Bovi and P. Giannozzi, *The Journal of Physical Chemistry C*, 2014, **118**, 29928-29942.
60. Y. Ju-Nam and J. R. Lead, *The Science of the total environment*, 2008, **400**, 396-414.
61. S.-D. Mo and W. Y. Ching, *Physical Review B*, 1995, **51**, 13023-13032.
62. T. A. Kandiel, A. Feldhoff, L. Robben, R. Dillert and D. W. Bahnemann, *Chemistry of Materials*, 2010, **22**, 2050-2060.
63. H. Chin Pao, R. O. M. Charles and J. M. James, *Aquatic Chemistry*, American Chemical Society, 1995.
64. J.-J. Yin, J. Liu, M. Ehrenshaft, J. E. Roberts, P. P. Fu, R. P. Mason and B. Zhao, *Toxicology and Applied Pharmacology*, 2012, **263**, 81-88.
65. C. Jin, Y. Tang, F. G. Yang, X. L. Li, S. Xu, X. Y. Fan, Y. Y. Huang and Y. J. Yang, *Biological Trace Element Research*, 2011, **141**, 3-15.
66. Q. Yu, H. Wang, Q. Peng, Y. Li, Z. Liu and M. Li, *Journal of Hazardous Materials*, 2017, **335**, 125-134.
67. M. Kleber, P. Sollins and R. Sutton, *Biogeochemistry*, 2007, **85**, 9-24.
68. M. Baalousha, *Science of The Total Environment*, 2009, **407**, 2093-2101.
69. J. J. Gulicovski, L. S. Čerović and S. K. Milonjić, *Materials and Manufacturing Processes*, 2008, **23**, 615-619.

70. M. Kosmulski, *Advances in Colloid and Interface Science*, 2016, **238**, 1-61.
71. M. Favaro, B. Jeong, P. N. Ross, J. Yano, Z. Hussain, Z. Liu and E. J. Crumlin, *Nature Communications*, 2016, **7**, 12695.
72. I. Siretanu, D. Ebeling, M. P. Andersson, S. L. S. Stipp, A. Philipse, M. C. Stuart, D. van den Ende and F. Mugele, *Scientific Reports*, 2014, **4**, 4956.
73. P. C. Himenz and R. Rajagopalan, *Principles of Colloidal and Surface Chemistry*, Tayler & Francis, 3 edn., 1997.
74. J. O. M. Bockris, A. K. N. Reddy and M. E. Gamboa-Aldeco, *Modern Electrochemistry 2A*, Springer US, 2000.
75. E. B. Zhulina, O. V. Borisov and V. A. Priamitsyn, *Journal of Colloid and Interface Science*, 1990, **137**, 495-511.
76. F. Lafuma, K. Wong and B. Cabane, *Journal of Colloid and Interface Science*, 1991, **143**, 9-21.
77. M. G. Carneiro-da-Cunha, M. A. Cerqueira, B. W. S. Souza, J. A. Teixeira and A. A. Vicente, *Carbohydrate Polymers*, 2011, **85**, 522-528.
78. R. Venditti, X. Xuan and D. Li, *Microfluidics and Nanofluidics*, 2006, **2**, 493-499.
79. A. V. Delgado, F. González-Caballero, R. J. Hunter, L. K. Koopal and J. Lyklema, *Journal of Colloid and Interface Science*, 2007, **309**, 194-224.
80. I. S. Grover, S. Singh and B. Pal, *Applied Surface Science*, 2013, **280**, 366-372.
81. S. Martin, M. Albert, C. Hai-Ping and B. Catherine, *ChemPhysChem*, 2015, **16**, 855-865.
82. W. Stumm, 1995, **244**, 1-32.
83. C. J. van Oss, *Current Opinion in Colloid & Interface Science*, 1997, **2**, 503-512.
84. L. M. Torres, A. F. Gil, L. Galicia and I. González, *Journal of Chemical Education*, 1996, **73**, 808.
85. E. W. Shin, J. S. Han, M. Jang, S.-H. Min, J. K. Park and R. M. Rowell, *Environmental Science & Technology*, 2004, **38**, 912-917.
86. A. A. Taha and S. A. A. Ghani, *Journal of Dispersion Science and Technology*, 2016, **37**, 173-182.

87. H.-K. Chung, W.-H. Kim, J. Park, J. Cho, T.-Y. Jeong and P.-K. Park, *Journal of Industrial and Engineering Chemistry*, 2015, **28**, 241-246.
88. X. Song, Y. Zhang, C. Yan, W. Jiang and C. Chang, *Journal of Colloid and Interface Science*, 2013, **389**, 213-219.
89. Z. Y. Yao, J. H. Qi and L. H. Wang, *Journal of Hazardous Materials*, 2010, **174**, 137-143.
90. E. E. Michaelides, *International Journal of Heat and Mass Transfer*, 2015, **81**, 179-187.
91. J. Gregory, *Advances in Colloid and Interface Science*, 2009, **147-148**, 109-123.
92. N. M. Kovalchuk and V. M. Starov, *Advances in Colloid and Interface Science*, 2012, **179-182**, 99-106.
93. S.-W. Bian, I. A. Mudunkotuwa, T. Rupasinghe and V. H. Grassian, *Langmuir : the ACS journal of surfaces and colloids*, 2011, **27**, 6059-6068.
94. R. F. Domingos, N. Tufenkji and K. J. Wilkinson, *Environmental Science & Technology*, 2009, **43**, 1282-1286.
95. K. L. Chen and M. Elimelech, *Journal of Colloid and Interface Science*, 2007, **309**, 126-134.
96. T. Tadros, in *Encyclopedia of Colloid and Interface Science*, ed. T. Tadros, Springer Berlin Heidelberg, Berlin, Heidelberg, 2013, DOI: 10.1007/978-3-642-20665-8_76, pp. 363-363.
97. C. Lourenco, M. Teixeira, S. Simões and R. Gaspar, *International Journal of Pharmaceutics*, 1996, **138**, 1-12.
98. Y. Zhang, Y. Chen, P. Westerhoff and J. Crittenden, *Water research*, 2009, **43**, 4249-4257.
99. C. L. Tiller and C. R. O'Melia, in *Colloids in the Aquatic Environment*, ed. J. Gregory, Elsevier, Oxford, 1993, DOI: <http://dx.doi.org/10.1016/B978-1-85861-038-2.50010-3>, pp. 89-102.
100. D. Dickson, G. Liu, C. Li, G. Tachiev and Y. Cai, *Science of The Total Environment*, 2012, **419**, 170-177.
101. B. Derjaguin and L. Landau, *Progress in Surface Science*, 1993, **43**, 30-59.
102. E. J. W. Verwey, *The Journal of Physical and Colloid Chemistry*, 1947, **51**, 631-636.
103. J. H. Adair, E. Suvaci and J. Sindel, in *Encyclopedia of Materials: Science and Technology*, eds. K. H. J. Buschow, R. W. Cahn, M. C.

- Flemings, B. Ilschner, E. J. Kramer, S. Mahajan and P. Veysseyre, Elsevier, Oxford, 2001, DOI: <https://doi.org/10.1016/B0-08-043152-6/01622-3>, pp. 1-10.
104. H. Ohshima, in *Colloid and Interface Science in Pharmaceutical Research and Development*, eds. H. Ohshima and K. Makino, Elsevier, Amsterdam, 2014, DOI: <https://doi.org/10.1016/B978-0-444-62614-1.00001-6>, pp. 1-28.
 105. A. I. Gómez-Merino, F. J. Rubio-Hernández, J. F. Velázquez-Navarro, F. J. Galindo-Rosales and P. Fortes-Quesada, *Journal of Colloid and Interface Science*, 2007, **316**, 451-456.
 106. J. Pátek, J. Hruby, J. Klomfar, M. Soucková and A. H. Harvey, *Reference Correlations for Thermophysical Properties of Liquid Water at 0.1 MPa*, 2009.
 107. Z. Abbas, J. P. Holmberg, A. K. Hellström, M. Hagström, J. Bergenholtz, M. Hasselöv and E. Ahlberg, *Colloids and Surfaces A: Physicochemical and Engineering Aspects*, 2011, **384**, 254-261.
 108. K. S. W. Sing, D. H. Everett, R. A. W. Haul, L. Moscou, R. A. Pierotti, J. Rouquerol and T. Siemieniowska, in *Handbook of Heterogeneous Catalysis*, Wiley-VCH Verlag GmbH & Co. KGaA, 2008, DOI: 10.1002/9783527610044.hetcat0065.
 109. H. S. E. and J. Kornelia, *Current Protocols in Protein Science*, 1998, **11**, 7.8.1-7.8.14.
 110. U. Nobbmann and A. Morfesis, *Materialstoday*, 2009, **12**, 52-54.
 111. E. A. Mun, C. Hannell, S. E. Rogers, P. Hole, A. C. Williams and V. V. Khutoryanskiy, *Langmuir : the ACS journal of surfaces and colloids*, 2014, **30**, 308-317.
 112. L. H. Allen and E. Matijević, *Journal of Colloid and Interface Science*, 1970, **33**, 420-429.
 113. R. B. Perry, *Journal of Chemical Education*, 1987, **64**, A328.
 114. H. Ohshima, *Journal of Colloid and Interface Science*, 1994, **168**, 269-271.
 115. Z. L. Wang, *The Journal of Physical Chemistry B*, 2000, **104**, 1153-1175.
 116. D. B. Williams and C. B. Carter, *Transmission Electron Microscopy - Part I: Basics*, Springer Science+Business Medi, New York, 2009.
 117. K. Fuwa, P. Pulido, R. McKay and B. L. Vallee, *Analytical Chemistry*, 1964, **36**, 2407-2411.

118. S. Ata, F. H. Wattoo, M. Ahmed, M. H. S. Wattoo, S. A. Tirmizi and A. Wadood, *Alexandria Journal of Medicine*, 2015, **51**, 19-23.
119. D. Van Der Spoel, E. Lindahl, B. Hess, G. Groenhof, A. E. Mark and H. J. C. Berendsen, *Journal of Computational Chemistry*, 2005, **26**, 1701-1718.
120. K. Vanommeslaeghe, E. Hatcher, C. Acharya, S. Kundu, S. Zhong, J. Shim, E. Darian, O. Guvench, P. Lopes, I. Vorobyov and A. D. Mackerell, *Journal of Computational Chemistry*, 2010, **31**, 671-690.
121. P. Bjelkmar, P. Larsson, M. A. Cuendet, B. Hess and E. Lindahl, *Journal of Chemical Theory and Computation*, 2010, **6**, 459-466.
122. S. Pradhan, J. Hedberg, J. Rosenqvist, C. M. Jonsson, S. Wold, E. Blomberg and I. Odnevall Wallinder, *PLoS ONE*, 2018, **13**, e0192553.
123. L. Krumina, G. Lyngsie, A. Tunlid and P. Persson, *Environmental Science & Technology*, 2017, **51**, 9053-9061.
124. T. Polubesova, S. Eldad and B. Chefetz, *Environmental Science & Technology*, 2010, **44**, 4203-4209.
125. M. Jaishankar, T. Tseten, N. Anbalagan, B. B. Mathew and K. N. Beeregowda, 2014, **7**, 60.
126. I. Sheet, A. Kabbani and H. Holail, *Energy Procedia*, 2014, **50**, 130-138.
127. J.-L. Gong, B. Wang, G.-M. Zeng, C.-P. Yang, C.-G. Niu, Q.-Y. Niu, W.-J. Zhou and Y. Liang, *Journal of Hazardous Materials*, 2009, **164**, 1517-1522.
128. G.-M. Zeng, X. Li, J.-H. Huang, C. Zhang, C.-F. Zhou, J. Niu, L.-J. Shi, S.-B. He and F. Li, *Journal of Hazardous Materials*, 2011, **185**, 1304-1310.
129. P. C. Redfern, P. Zapol, L. A. Curtiss, T. Rajh and M. C. Thurnauer, *The Journal of Physical Chemistry B*, 2003, **107**, 11419-11427.
130. F. Loosli, P. Le Coustumer and S. Stoll, *Water research*, 2013, **47**, 6052-6063.
131. A. R. Petosa, D. P. Jaisi, I. R. Quevedo, M. Elimelech and N. Tufenkji, *Environmental Science & Technology*, 2010, **44**, 6532-6549.